Hypogenic speleogenesis, late stage epigenic overprinting and condensation-corrosion in a complex cave system in relation to landscape evolution (Toirano, Liguria, Italy)

Hypogenic speleogenesis, late stage epigenic overprinting and condensation-corrosion in a complex cave system in relation to landscape evolution (Toirano, Liguria, Italy)

Andrea Columbu ([a])*, Philippe Audra ([b]), Fernando Gázquez ([c]), Ilenia M. D'angeli ([a]), Jean-Yves Bigot ([d]), Gabriella Koltai ([e]), Roberto Chiesa ([f]), Tsai-Luen Yu ([g]), Hsun-Ming Hu ([g]), Chuan-Chou Shen ([g]), Cristina Carbone ([h]), Vasile Heresanu ([i]), Jean-Claude Nobécourt ([d]), Jo De Waele ([a])

([a]) Dipartimento di Scienze Biologiche, Geologiche e Ambientali, Università di Bologna, Italy, andrea.columbu2@unibo.it, dangeli.ilenia89@gmail.com, jo.dewaele@unibo.it

([b]) University Côte d'Azur, Polytech'Lab - UPR 7498, Nice, France, Philippe.AUDRA@univ-cotedazur.fr

([c]) Department of Biology and Geology, University of Almeria, Spain, f.gazquez@ual.es

([d]) French Association of Karstology (AFK), France, jeanbigot536@gmail.com, jcnobecourt@free.fr

([e]) Institute of Geology, University of Innsbruck, Innrain 52, 6020, Innsbruck, Austria, gabriella.koltai@uibk.ac.at

([f]) Gruppo Speleologico Cycnus, Toirano, Italy, bobchurch69@gmail.com

([g]) High-Precision Mass Spectrometry and Environmental Change Laboratory (HISPEC), Department of Geosciences, National Taiwan University, Taipei 10617, Taiwan ROC, d00224009@g.ntu.edu.tw, hsunming.hu@gmail.com, river@ntu.edu.tw

([h]) DISTAV, Università degli Studi di Genova, C.so Europa 26, 16132 Genova, Italy, cristina.carbone@unige.it

([i]) CINaM, CNRS – Aix Marseille University, Campus de Luminy, case 913, 13288 Marseille cedex 9, France, heresanu@cinam.univ-mrs.fr

(*) corresponding author

Abstract

The Toirano karst system is located in the Ligurian Alps (north Italy), around 4.5 km inland from the coastline and carved in Middle Triassic dolostone. It comprises five cave levels over a 154 m altitudinal range, specifically Ulivo (340 m a.s.l.), Colombo (247 m a.s.l), Upper Santa Lucia (215 m a.s.l.), Lower Santa Lucia (201 m a.s.l.) and Bàsura (186 m a.s.l.) caves. The system is active at lower altitudes, as testified by the thermal spring currently located at 70 m a.s.l. along the Varatella valley. Speleogenesis was attributed to the action of epigenic processes by other authors. However, the extraordinary geodiversity of the underground morphologies and deposits are at odds with this interpretation. Accordingly, this work investigates the genesis of the Toirano karst system, in relation to the landscape evolution of the surrounding area. A detailed morphological and mineralogical investigation of cave geoforms and deposits, together with the presence of an active low thermal sulphide spring on the Varatella valley and only ~100 m below the Bàsura Cave, sustain the hypothesis of a hypogene origin of the caves. This work shows that most of the caves formed close to the former water table (base) level, in turn determined by the mean sea level. Geochronological analyses, including U/Th (n = 13) and cosmogenic burial (n = 1) dating, together with an estimated incision rate of the Varatella valley of around 0.1 mm y^{-1}, have allowed to assess the age of the highest cave (Ulivo) at around 2.7 Ma, Colombo at ~1.8 Ma, Upper Santa Lucia at ~1.5 Ma, Lower Santa Lucia ~1.3 Ma and Bàsura at ~1.2 Ma. Estimated palaeotemperature attained through isotope analyses and fluid inclusions on speleothems suggest that the temperature of rising waters was lower than 50 ˚C and possibly ranging between ~12 and ~20˚C, indicating that hydrothermal fluids were not the main driver of speleogenesis, at least in the late speleogenic phases. Additionally, sulphuric acid speleogenesis by-products were not identified. Accordingly, hypogenic speleogenesis occurred because of the action of low temperature CO_2-rich rising fluids.

A late stage of epigenic speleogenesis has been detected because of the clear evidences of condensation-corrosion morphologies, occurred since ~150 ka (possibly earlier) when caves were finally connected to the surface because of valley enlargement. Besides uncovering the genesis of the Toirano karst system, this study demonstrates that the combination of local geology, surface vs underground geomorphological observations, climate change vs landscape evolution evaluation and geochemical data is of key importance for interpreting subsurface land-shaping processes.

Keywords

Speleogenesis, hypogene karst, dating, stable isotopes, cave geomorphology

1. Introduction

The geological non-specialist community, as well as the public, is often unaware of the multiple processes leading to cave formation. Indeed, speleogenesis is too often considered as an epigenic process (*sensu* Ford and Williams, 2007) only. In this circumstance, the hydrogeological circulation ultimately leading to cave excavation is sustained by surface water infiltrating the bedrock. The action of bedrock dissolution in phreatic, epiphreatic, and vadose conditions along the water table is also often taken for granted. Indeed, epigene caves are often arranged in levels, which record the former base level (water table) stillstands (Palmer, 1987), and can thus help in unravelling the landscape evolution of the areas in which they were carved (Calvet et al., 2015; Columbu et al., 2015, 2017; Bella et al., 2019; Ballesteros et al., 2019; Pennos et al., 2019; Nehme et al., 2020). However, cave formation does not exclusively occur through epigenic speleogenesis. An increasing body of evidence suggests that many caves formed by hypogene processes (*sensu* Klimchouk, 2007), which imply upward recharge from a deep route rather than epigenic input (Plan et al., 2012; Tisato et al., 2012; Klimchouk et al., 2017; Pérez-Mejías et al., 2019; Klanica et al., 2020). Rising fluids are rich in CO_2 and/or H_2S, and can be sourced from deep hydrothermal activity (Temovski et al., 2013). Hypogene caves can also form at former water table levels, such as in the case of thermal caves (Léel-Őssy, 2017), and particularly in sulphuric acid (SAS) caves, where degassing of H_2S and oxidation is most efficient at or immediately above the water surface (De Waele et al., 2016; D'Angeli et al., 2019a). Hypogene-SAS caves are reliable indicators of past water table levels and can help in determining base level changes, and especially uplift rates (or related downcutting rates in adjacent valleys) (Piccini et al., 2015; De Waele et al., 2016; D'Angeli et al., 2019b).

The common epigenic origin is usually supported by the current presence of water streams in caves and/or the "rounded" passages interpreted as phreatic conduits (Sauro et al., 2020). However, the modern streams and the actual shape of natural underground conduits can be the result of recent geological events; the effective processes leading to cave formation must be traced further in the past, i.e. when the initial fluids started enlarging the most permeable pathways, leading to the selection of the most effective drainage routes (Ford and Williams, 2007; Palmer, 2007). Furthermore, the geomorphological evidences of ancient speleogenesis can be partially lost because of weathering, speleothem deposition, sedimentation, collapses, human activity, etc. (Sauro et al., 2019). There are processes such as condensation-corrosion, boosted by the presence of guano and/or warm and moist air circulation in caves, which are greatly underestimated in the shaping of caves (Audra et al., 2016; Cailhol et al., 2019; Dandurand et al., 2019). These processes, instead, can be extremely important in the late speleogenetic stages, especially when cave passages become largely opened to the surface, concurrently erasing evidences coming from the deeper past. Accordingly, the study of cave formation needs an accurate interpretation of underground morphologies (conduit shape, size, geometries; wall, ceiling and floor features; chemical precipitates and sediments; etc.), which should also be supported by geochemical and stratigraphic analyses of cave deposits (speleothems vs. sediments), considerations about the bedrock discontinuities (faults, lineaments, bedding, etc.), the geological status of the area (active tectonic, uplifting vs. subsidence, etc.), and evaluations about surface dynamics related to climate and landscape evolution (De Waele et al., 2009; Audra and Palmer, 2015; Columbu et al., 2015, 2017).

Additionally, speleogenetic processes must be pinpointed in time, thus dating is a key for anchoring underground processes to a coherent geochronology (Sasowsky, 1998).

The Toirano karst system in Liguria, Northern Italy, is developed along a series of close-to-horizontal cave passages and an impressive variety of underground morphologies, as much as probably making it the Italian show cave with the highest geodiversity. Its features challenge a straightforward interpretation of its formation, although past local investigators have considered epigene speleogenesis as the main player. However, the presence of a nearby thermo-mineral spring suggests a possible influence of a deep flow component, and substantial differences in morphologies are indicative of processes associated to confined areas vs passages strongly influenced by a connection to the surface, such as bat-related biocorrosion and condensation-corrosion. Here, the in-detail investigation of cave morphologies and stratigraphy, U/Th dating and stable isotope analyses of speleothems and cosmogenic burial dating of sediments, support a novel interpretation of the main processes leading to speleogenesis, occurring in a dynamic environmental context of changing climate and landscape.

We take the Toirano karst system as an example of an enigmatic case study to suggest a guideline in the investigation of cave evolution, based on a correct interpretation of underground morphologies, sustained by geochemical analyses, anchored in time by dating and coherently integrated with surface events. Our results allow reconstructing the evolution phases of the cave system during the Quaternary, witnessing profound changes in the surrounding landscape.

2. Study area

The Toirano karst system develops along the lower slopes of Mt. Carmo di Loano (1389 m asl), half a kilometre north of the small village of the same name (Savona Province, Liguria Region, north-western Italy) (Fig. 1).

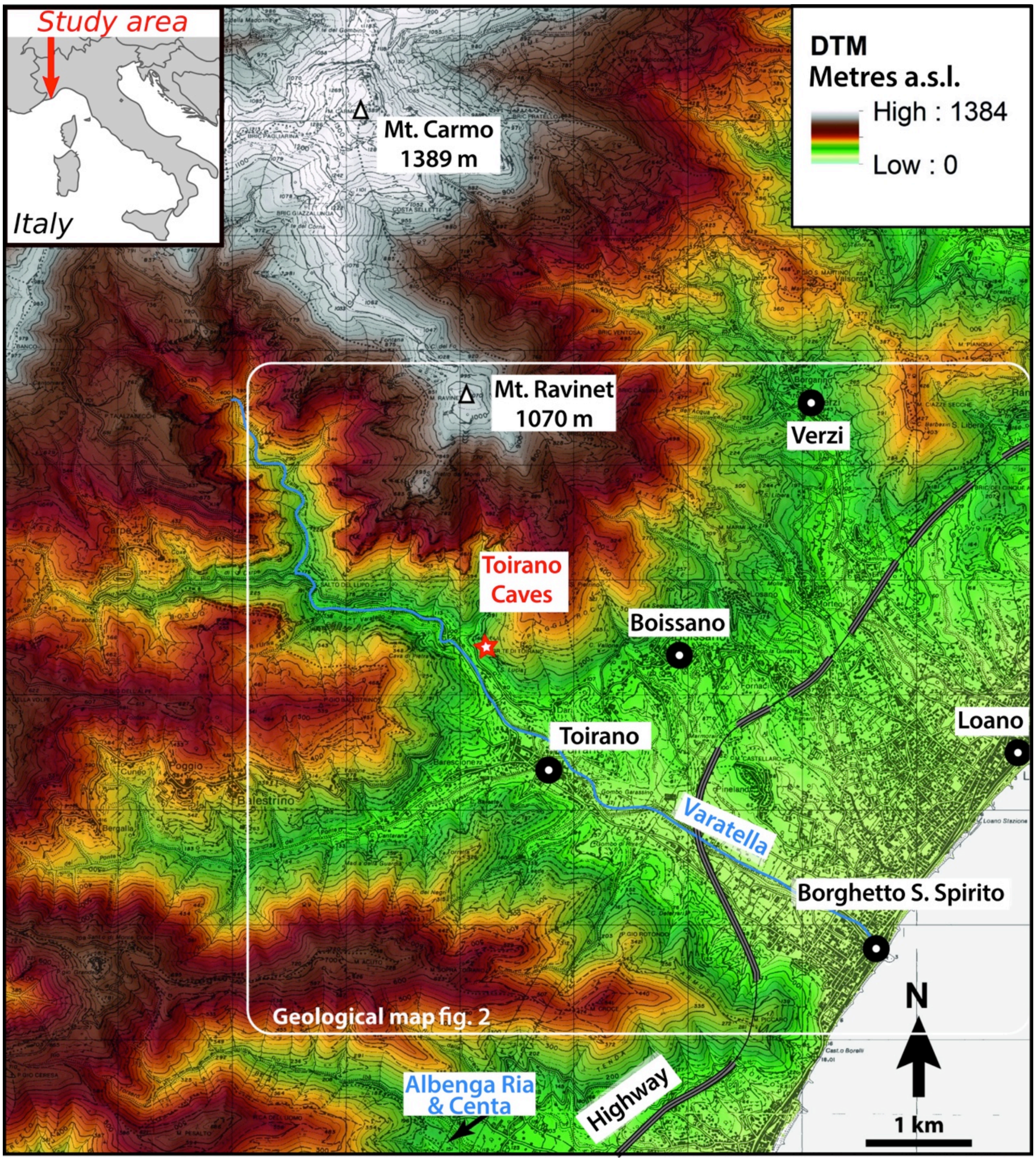

Fig. 1. Location of the study area and the Toirano Caves in Liguria, NW Italy. Refer to Fig. 2 for the geological setting.

The caves develop in the slopes on the hydrographic left of the Varatella torrent, at the outlet of its gorges, upstream of the coastal plain; the shoreline is located only 4.5 km downstream from the caves. This area belongs to the Briançonnais domain of the Ligurian Alps, being part of a complex dome structure dipping here 20-30° toward the NE (Boni et al., 1971; Cavallo, 2001; Fig. 2). The *San Pietro dei Monti* Formation (Fm.) (Middle Triassic) constitutes the main local unit. Although mainly composed by dolostone, it presents a more calcareous lower formation (*Costa Losera Fm.*), in which most caves are carved. Toward the south, the carbonate rocks are interrupted by a NE-SW normal fault with a vertical offset of at least 200 m, that places the Middle Triassic dolostones in contact with the quartzite of the *Ponte di Nava* Fm. (Lower Triassic in age) (Fig. 2) (Menardi Noguera, 1984; Cavallo, 2001).

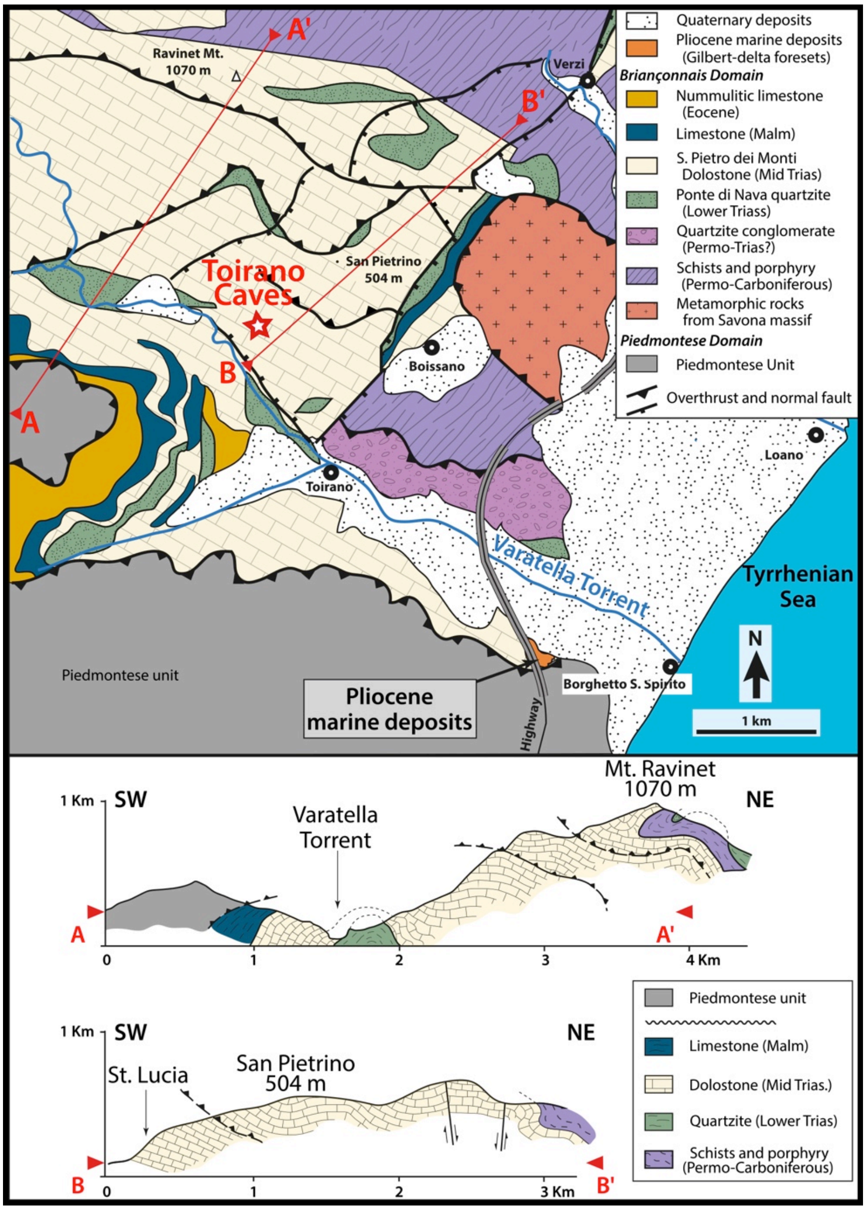

Fig. 2. Simplified geological map and profiles of the studied area (after Boni et al., 1971; Menardi Noguera, 1984). Note the marine Pliocene deposits to the south.

It is along this major tectonic contact that the thermal spring of Toirano is located, on the hydrographic right side of the Varatella torrent and at an altitude of 70 m asl (Fig. 3). This spring has a rather high mean discharge of 100 $L \cdot s^{-1}$ and delivers waters of 22-23 °C, with a slightly basic pH (7.2-7.4) and moderate mineralisation (ca. 600 µS/cm at 20 °C, hardness of 23 °F); it consists in a bicarbonate-calcium type water with low concentration in sulphates (25-37 mg L^{-1} SO_4^{2-}) (Calandri, 2001). These hydrogeochemical characteristics are stable year-round and even after important rain and flood events, which would exclude significant mixing with shallow meteoric water and surface runoff from the Varatella torrent. The isotopic signature of the thermal spring ($\delta^{18}O$ = -6,9 ‰ vs. -5,8 ‰ at the coast), points toward a mean altitude of its catchment at around 400 m a.s.l, corresponding to a surface of at least 4 km^2 along the slopes of Mt. Carmo (Cavallo, 1990).

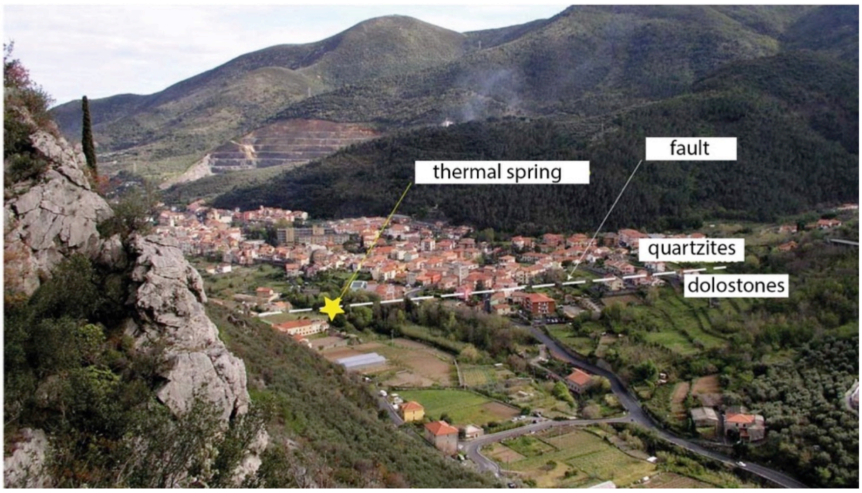

Fig. 3. View downstream on Toirano village and on the Varatella torrent from the entrance of Colombo Cave. The Mediterranean shoreline is located 4.5 km southward, behind the hills (Photo J.-Y. Bigot).

The Varatella torrent generated fluvial terraces that can be traced up to an altitude of ca. 100 m asl (Fanucci et al., 1987). In the neighbouring Ria of Albenga (5 km south of the study area, Fig. 1) there are remnants of two levels of Lower Pliocene shorelines located at 280-310 and 380-420 m asl, showing a Plio-Quaternary uplift of the mountain front of at least 350-400 m (Marini, 2004). Offshore, these Pliocene marine deposits, several hundreds of metres thick, are burying the deeply-incised Messinian canyon of the Centa River (Clauzon et al., 1996; Soulet et al., 2016). In the Varatella valley itself, Pliocene remnants are very scarce, limited to a conglomerate outcrop in a small plateau (45 m asl) at the outlet of the highway tunnel (Boni et al., 1971, Fig. 2). Its visible part displays an inclined layer of cemented angular limestone blocks originating from the local hill, resting on a sand bed. This conglomerate corresponds to inclined foreset beds of the Pliocene Gilbert-type delta filling the Messinian canyon of the Varatella river. This canyon can be traced offshore of Borghetto San Spirito, where it flowed together with the Centa Messinian canyon originating from the larger valley of Albenga (Soulet et al., 2016). Apart from these conglomerates, there is no indication of the inland extension of the Messinian Varatella canyon, which might have been uplifted and probably eroded. Currently, in Toirano, the Varatella torrent flows on the quartzite bedrock (Fig. 2).

Climate in Toirano is mild Mediterranean and maritime, warm and temperate, with an average annual temperature of 14.3 °C (mean minimum of 6.6 °C in January, mean maximum of 22.6 °C in July); annual rainfall is 830 mm with no pronounced wet season, while June and August are essentially dry.

The Toirano karst system is composed of Ulivo Cave (*Grotta dell'Ulivo*, 337 m asl, 27 m long), Colombo Cave (*Grotta di Colombo*, 247 m asl, 310 m long), Upper Santa Lucia Cave (*Grotta di Santa Lucia Superiore* or Sanctuary Cave, 215 m asl, 378 m long), Lower Santa Lucia Cave (*Grotta di Santa Lucia Inferiore*, 201 m asl, 778 m long) and the Bàsura Cave (*Grotta della Bàsura*, 186 m asl, 890 m long) (Chiesa, 2007; Gruppo Speleologico Cycnus and Delegazione Speleologica Ligure, 2001) (Fig. 4). A XV-XVI century church occupies the entrance hall of Upper Santa Lucia Cave; the cave walls are decorated by pilgrims signatures since this time.

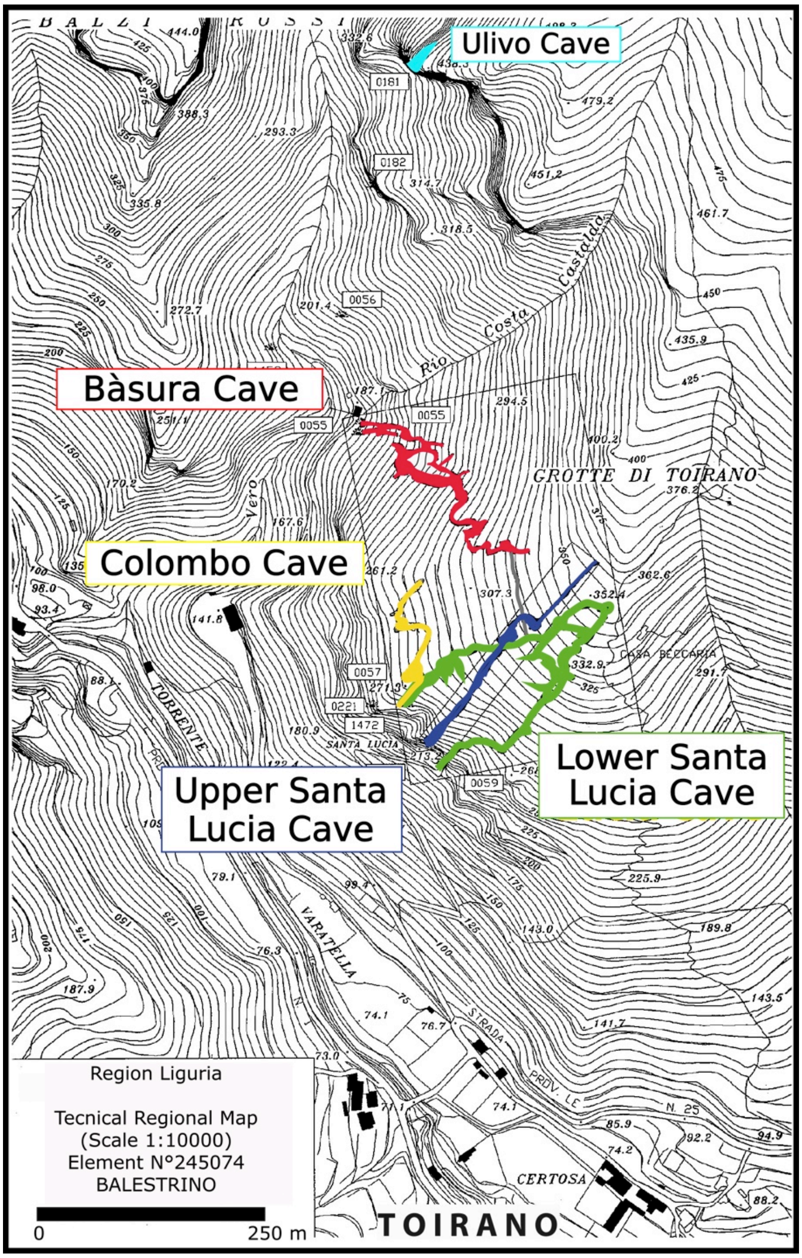

Fig. 4. Location of Toirano caves. The thermal spring is located nearby Certosa (see Fig. 3).

Bàsura Cave owes its celebrity because of the presence of ancient human footprints, first believe to be of Neanderthal, but later shown to be of early Homo Sapiens groups (Citton et al., 2017); it was opened to the public in 1953, and in 1967 a 110-m-long artificial tunnel connected Bàsura with Lower Santa Lucia Cave (Gruppo Speleologico Cycnus and Delegazione Speleologica Ligure, 2001). The tunnel has allowed discovering some new natural cave passages that would otherwise have remained unknown, since they do not have natural access. The construction works have emptied the lake that was present in the *Antro di Cibele* in the lowest part of the known Bàsura passages. The drying out of this lake has generated an important exchange of atmospheric masses between different cave branches, starting the circulation of large quantities of air in the cave environment, a process that was previously lacking.

Sarigu (2001) and Calandri (2001) have described the caves of the area from a geological, structural and geomorphological point of view, and gave the first detailed speleogenetic hypothesis. The caves are often characterised by long passages with very low inclination, carving inclined strata. These close-to-horizontal passages have probably developed along the former water table position. The direction of the cave passages is greatly controlled by the main fracture sets in the region with typical NE-SW directions (60% of all fractures), which are associated to the important uplift phases of Pliocene age, and minor components in the N-S (15%) and W-E directions (25%) (Sarigu, 2001). Most authors attribute cave formation to the Pliocene, related to the intense uplift of the region and the opening of the ENE-WSW fractures (Sarigu, 2001), although some authors even mention a start of cave-forming processes during the Lower Miocene (Fanucci, 1985).

3. Methods

We visited Toirano several times between 2015 and 2019 to carry out geomorphological observations and sampling in Bàsura, Lower and Upper Santa Lucia and Colombo caves. Sampling locations are reported in Fig. 5, whilst Figs. 6-9 report the most significant cave morphologies. Sediments and morphological features were considered within their spatial and stratigraphic relations, in order to attribute a relative chronology. Following our conservational purposes (Columbu et al., 2020), almost all samples were taken from fragments found broken on the ground, result of the constructional works outlined above.

Several mineral deposits showing peculiar characteristics at naked eye (i.e. colour, fabric, texture, morphology and stratigraphic location, see Tab. 1 for these observations and sampling location) were sampled in Colombo (n = 7), Lower Santa Lucia Cave (n = 10) and Bàsura (n = 5), and analysed with classical techniques X-Ray Diffractometry (XRD) and Scanning electron microprobe (SEM) analyses at Genova University (Italy) and at CINaM (CNRS - Aix-Marseille University, France. Full details on mineralogical analytical methods can be found in Audra et al. (2019). These analyses aim to better understand the processes driving the deposition of such a variety of secondary chemical deposits.

A sample of quartz- and feldspar-containing sands have been collected for Al-Be cosmogenic burial dating at the ASTER AMS National Facility (CEREGE-CNRS, Aix Marseille University, France). This is a well-established dating technique in karst-related studies, and full analytical details can be found in Bella et al. (2019). The sampling site is located 50 m from the entrance of Colombo Cave, shielded by a vertical rock thickness of at least 100 m, therefore no post-production was taken into account in the burial age calculations. Indeed, in deeply incised mountain torrents like the study area, production rates are not that influenced by the sourcing altitude because of the screening effect. We assume that the samples were exposed at the surface over long times accumulating nuclide concentrations, which started decreasing by radioactive decay once the sediments were buried in the caves. We used spallation production rates of 4.02 at/g/a for ^{10}Be (Borchers et al., 2016), which are assumed to be constant over time and scaled for latitude and elevation (Stone, 2000). Muon contributions were scaled following Braucher et al. (2011). The ^{26}Al/^{10}Be production ratio induced by the standardisation used at ASTER (SM-Al-11/STD11) is 6.61 ± 0.50. Only one age was produced by this method.

Fragments of speleothems have been dated by the U-series method at the High-Precision Mass Spectrometry and Environmental Change Laboratory (HISPEC) of the National Taiwan University following established protocols (for detailed methods see Shen et al., 2012 and Columbu et al., 2019). A total of 13 ages were produced, targeting different speleothems such as: i) flowstones; ii) stalagmites; and iii) subacqueous mammillary and pool calcite, equally distributed in the four explored caves (see Tab. 2 for sampling sites and typology of dated speleothems). U-Th ages are here applied to estimate the minimal age of the caves, as well as give a broad temporal indication for different statuses of the underground conduits (i.e. vadose vs. subaqueous speleothems), as in Gázquez et al. (2018). Raw age calculations were executed by using half-lives, given in Cheng et al. (2013) and then corrected by assuming an initial $^{230}Th/^{232}Th$ atomic ratio of $4.4 \pm 2.2\times10^{-6}$. Ages are provided, throughout the text, by the ka notation (ka = thousand years before present).

A double-polished thin section has been prepared to study a calcite raft from Bàsura Cave (TO19 from Cibele room) for fluid inclusion petrography following the methods described in Krüger et al. (2011). The arrangement and characteristics of fluid inclusions are here taken as indication of the temperature of parent water depositing the raft.

Finally, stable isotopes of oxygen and carbon ($\delta^{18}O$ and $\delta^{13}C$ standardised to Vienna Pee Dee Belemnite, VPDB) in calcite were measured at the University of Cambridge (UK) and Almeria (Spain) with a precision better than 0.1‰ (for details see Gázquez et al., 2018). Sampling was carried out in Bàsura (n = 6) and Colombo (n = 1) caves, with the aim of targeting those speleothems that could have potentially recorded signals of past hydrothermal activity. Indeed, $\delta^{18}O$ has been used here to estimate the water temperature during calcite precipitation. This is because the $^{18}O/^{16}O$ fractionation factor between the mineral and the solution ($\alpha_{calcite-water}$) is sensitive to temperature (Tremaine et al., 2011). This relationship is given by the expression (eq. 1):

$$1000 \ln \alpha_{calcite-water} = 16.1\ (10^3\ T^{-1}) - 24.6$$

where T is temperature (Kelvin degrees) and $\alpha_{calcite-water}$ is (eq. 2):

$$\alpha_{calcite-water} = \frac{\delta^{18}O_{calcite} + 1000}{\delta^{18}O_{water} + 1000}$$

In short, the $\delta^{18}O_{calcite}$ depends on the water temperature and $\delta^{18}O_{water}$ at the time of mineral precipitation. For calculations of palaeo-water temperatures in the Toirano caves we used: 1) the range of $\delta^{18}O_{calcite}$ obtained from the Toirano samples and 2) a $\delta^{18}O_{water}$ of -5.8‰ (V-SMOW), in line with the modern local mean values of $\delta^{18}O_{water}$ in rainfall (Cavallo, 1990); however, because the $\delta^{18}O_{water}$ of palaeo-water is unknown and may have changed with time as a result of varying climate, we used a range of ±0.5‰ for calculations.

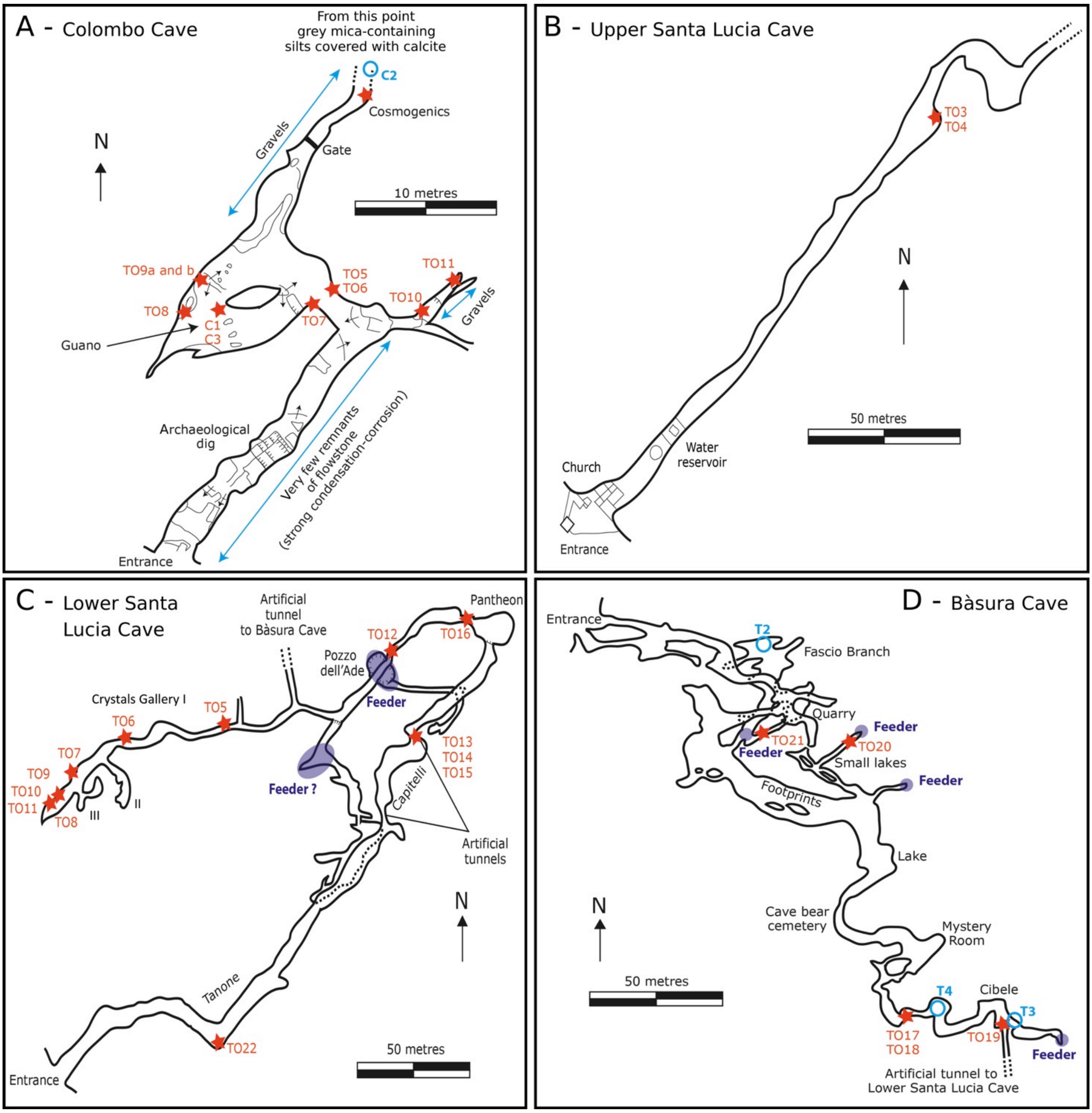

Fig. 5. Simplified plan view of Colombo Cave (A), Upper Santa Lucia Cave (B), Lower Santa Lucia Cave (C) and Bàsura Cave, reporting sampling (Survey courtesy of Gruppo Speleologico Cycnus and Delegazione Speleologica Ligure, 2001). Blue circles correspond to calcite samples collected for stable isotopes. Other samples are represented by red stars.

4. Results

4.1. Cave morphology and deposits

The caves and their deposits will be described starting from the highest (Colombo Cave) to the lowest (Bàsura Cave). Simplified plan views and locations of the samples are reported in Fig. 3. The small Ulivo Cave, located almost 100 m above Colombo has not been investigated. However, its large portal opening to a short 27 m-long passage is here considered as the highest cave level of the system.

4.1.1. Colombo Cave

Colombo Cave opens at 247 m asl. The wide entrance passage was used during prehistoric times, and a 4.5 m-deep archaeological excavation pit is present 10 m from the entrance (Fig. 6B). 25 m from the entrance, the passage opens in a large room of 10 m wide. In the bend of the passage, some smaller ascending galleries open to the east. The room then turns into a more-narrow passage towards the NE, where the cave continues for over 250 m in well decorated and faintly active (wet) passages. The passage ends on a sediment plug, thus the morphology of the conduit and the type of flow at the origin of the initial passage is not visible. This part was discovered after opening a flowstone plug that only left a centimetre-space for air circulation. Nowadays a gate closes this branch for conservation purposes.

The walls of the entrance passage and the main room have an overall smooth and wavy appearance. The roofs are sculpted by cupolas and ascending channels, some are highlighted by the presence of orange-coloured sediments (Fig. 6C). The main room is dominated by a large rock pillar standing at its centre, being larger at its top and narrowing toward the floor (Fig. 6F). Along the archaeological dig, the stratigraphy shows angular elements (cryoclastic material that has almost not been moved from where it was formed). U/Th and ESR dating at 76-70 ka assign the lower part of the excavation to Marine Isotope Stage (MIS) 5 (Pirouelle, 2006). Patches of coarse alluvial sediments can be seen stuck on the limestone walls (Fig. 6A). Their rounded pebbles, made of both local dolostone and allogenic material (quartzite, green schist), are up to 5 cm in diameter, and they are cemented in a reddish matrix containing mica and quartz. Their source can be traced upstream in the Varatella valley, where quartzite, polygenic conglomerates, and various metamorphic rocks crop out (Boni et al., 1971) (Fig. 2). Similar alluvial deposits, but smaller size, are present in the small ascending passage. In the inner portion of the cave, there are pockets of sands of similar composition (Fig. 6C, H; TO6). The decrease of grainsize toward the cave interior testifies that water, which deposited this material, came from the entrance. This material has been used for Al-Be burial dating (Tab. 3). Remnants of old corroded flowstones can be seen here and there along the walls and have been sampled for U/Th dating (Tab. 2 and Fig. 6). On the contrary, shallow pools with active speleothems are located behind the gate, where a rather important air circulation is present. The floor of the central room is covered by dark bat guano deposits, most of which seems to be rather old (Fig. 6F). Yellowish crusts (samples C1, C3, TO9a; Fig. 6G) and flowery overgrowths have shown the presence of typical sulphate and phosphate minerals of guano decay, including gypsum, ardealite, and newberyite, whereas leucophosphite was detected in samples TO9a and TO9b (Audra et al., 2019). In the ascending passage, a brown crust (TO11) covering the carbonate wall is composed of apatite (Tab. 1).

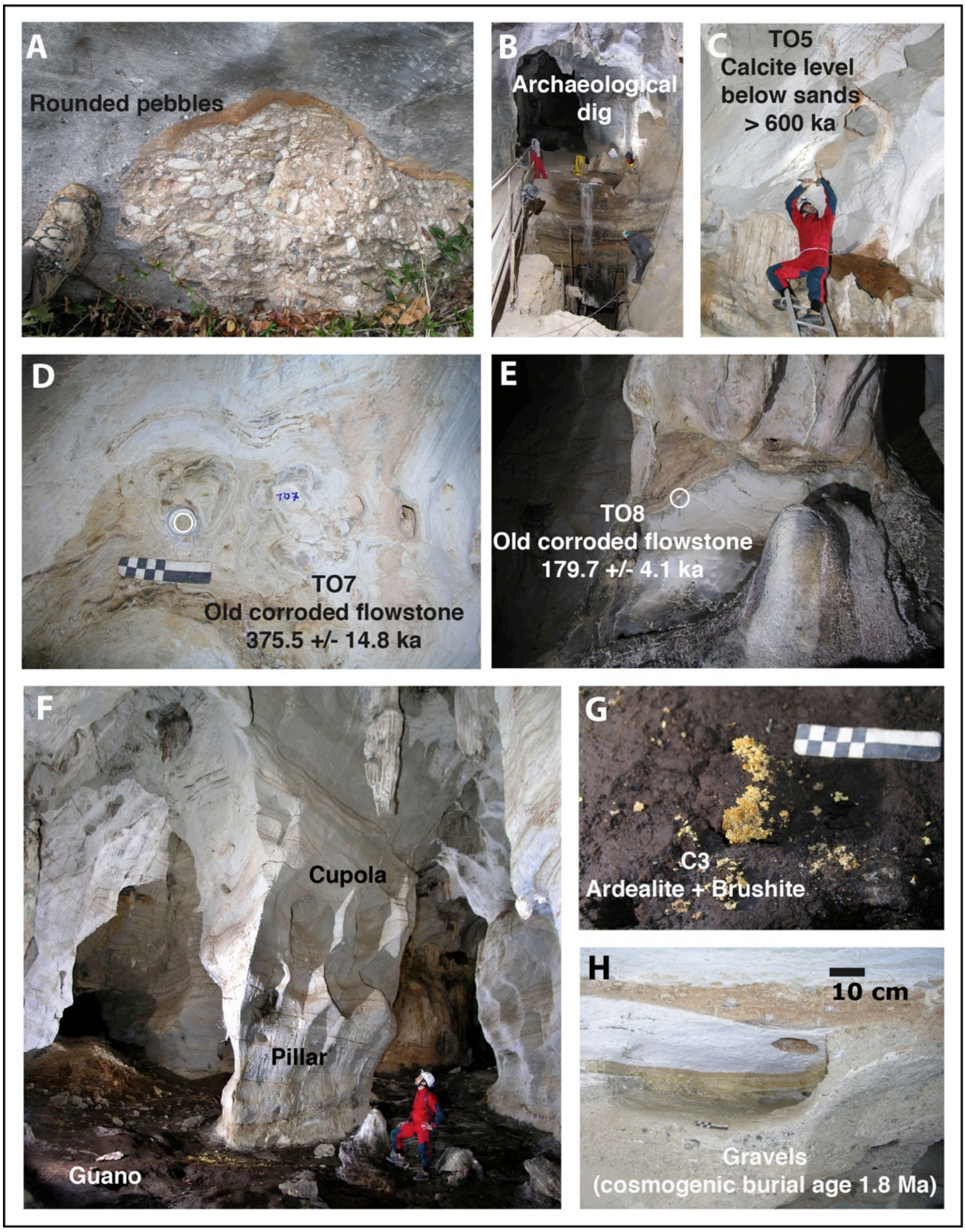

Fig. 6. Morphologies and deposits in Colombo Cave (Photos by Jean-Yves Bigot): A. Cemented pebble deposit in a reddish loamy matrix, found outside at the entrance of Colombo Cave; B. The archaeological excavation pit a few metres from the entrance; C. Rising cupolas filled with a calcite coating (TO5) and a sandy deposit (TO6); D. Old corroded flowstone (TO7) at the entrance of the large room; E. Old flowstone (TO8) sampled on the western wall of the room; F. Overview of the central large room with the pillar, cupola on the ceiling, and abundant guano deposits; G. Yellowish secondary minerals on guano (ardealite and brushite); H. Gravels sampled for cosmogenic burial dating.

4.1.2. Upper Santa Lucia Cave

The first 50 m of the large entrance are occupied by the still active church. Visits were initially possible using candles, then carbide lamps, the reason why the floor and walls have become blackened by soot (Fig. 7C-D). The cave continues behind the altar. The passage ends in an old flowstone, which has been damaged by explosives, probably in the hope of finding a continuation of the cave. These "exploration" attempts however failed. Consequently, the characteristics of the original passage feeding the cave cannot be investigated. Most of the inner part of the cave shows strong effects of condensation-corrosion as evidenced by smoothed walls and visible deep-inner rings of flowstones (Fig. 7C). The roof is characterised by a never-ending network of interpenetrating cupolas (Fig. 7D). In places, at the vertical of ceiling pendants where condensation water concentrated, large dripping pots are developed (Fig. 7E). The floor is covered with patches of old guano (Fig. 7D), and it is clear that large bat colonies inhabited the cave in the past. We sampled an old corroded flowstone (TO3, 407.6 ±22 ka) and a slightly younger rimstone (TO4, 343.0 ±10.4 ka; Fig. 7F, Tab. 2).

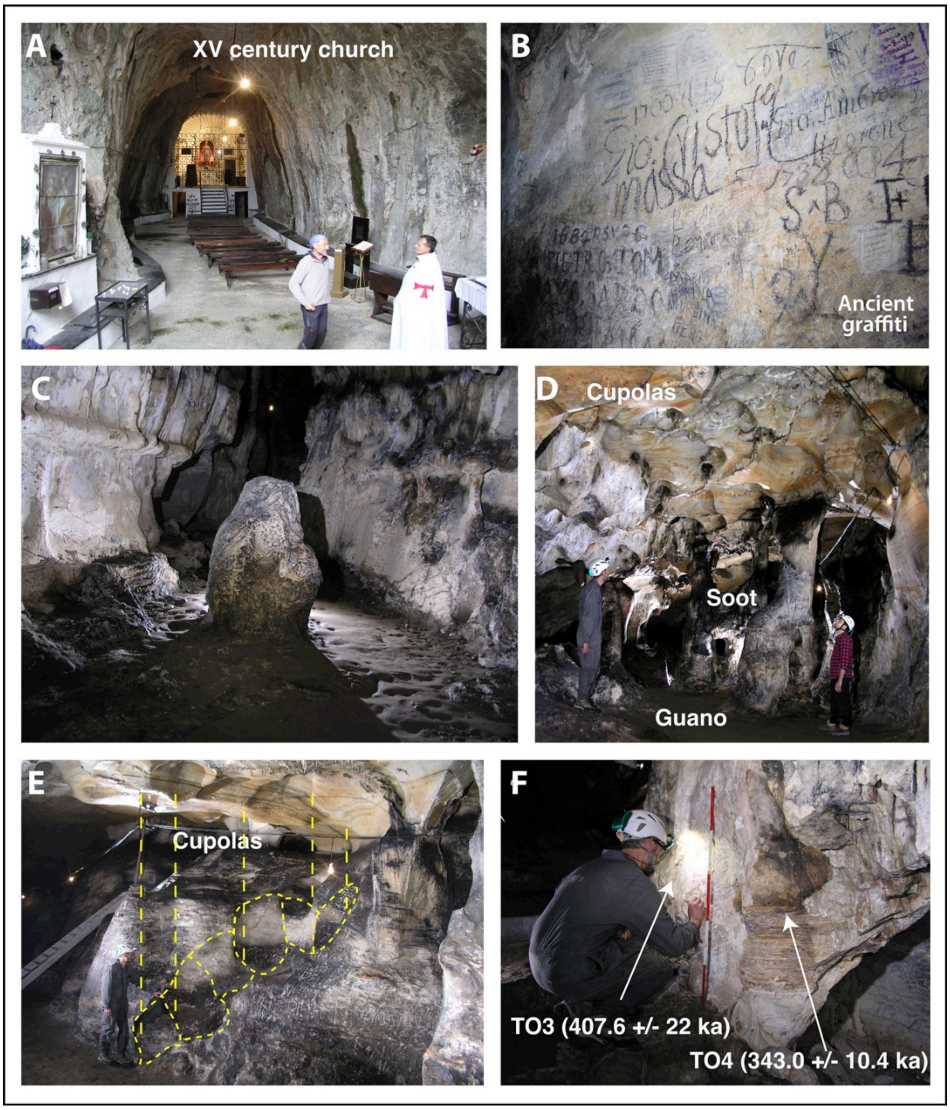

Fig. 7. Morphologies in Upper Santa Lucia Cave (Photos by Jean-Yves Bigot): A. The XV century church in the wide entrance part of the cave; left to the altar, a door closes the inner part; B. Graffiti on the walls in the inner cave (note writings of year 1687 to the left); C. Strongly corroded stalagmite (1.5 m tall) with growth rings highlighted by soot veneer. Lateral calcite shelves, similar to TO4, recording an ancient pool level, are visible on the walls; D. The final part of the cave with corroded speleothems, coalescing cupolas, remnants of black soot on the walls, and a floor covered with old bat guano; E. Biocorrosion cupolas (derived from bat and guano) and dripping-pots, which are developing at the vertical of ceiling pendants that concentrate condensation runoff; F. The sampled old flowstone (TO3) and the younger rimstone deposits (TO4).

4.1.3. Lower Santa Lucia Cave

Lower Santa Lucia Cave is located at 201 m asl, 14 m below and slightly south of the Upper Santa Lucia Cave. It splits into five distinct parts (Fig. 5C): the 200 m-long entrance gallery (*Tanone*), entering into the massif following a NE orientation; the *Capitelli* (the "Capitals") of the same direction; the Pantheon, a large descending circular chamber; the gallery of Pozzo dell'Ade, turning back SW toward the valley and from which depart two smaller side passages (Crystals Gallery II and III) and the artificial tunnel connecting with Bàsura Cave; and the Crystals Gallery I of the same SW direction.

The entrance gallery (*Tanone*), is a perfectly horizontal over 5 m wide and 10 m high passage, with smooth corroded walls displaying a powdery dry aspect, and with almost no speleothems, except for a few old corroded and massive flowstones. It looks more like a mining tunnel than a natural cave (Fig. 8A). The *Capitelli* is isolated behind a passage opened through a calcite plug, now equipped with a door that maintains the confinement of the inner part from the external air. Behind this confining door, the cave appears as a completely different environment with respect to the outer part, showing smaller dimensions and abundant flowstones. The *Capitelli* displays mushroom-like speleothems, with a series of shelfstone levels growing at different heights above the cave floor, culminating in a more extensively developed shelfstone level at 1.7 m height, forming the hats of the mushrooms (Fig. 8C). The horizontal *Capitelli* passage then opens into Pantheon, a large descending circular room, which is covered with calcite crystals (Fig. 8G). The room is decorated with large stalagmites and stalactites, all showing a white and powdery corroded surface towards the interior of the cave and deposition of reddish fines (toward the entrance) on the other side. The warm and wet air flowing from inside the cave toward the entrance causes this corrosion. This airflow is forced to pass a narrower passage, and this compression causes condensation on the speleothem sides facing toward the Pantheon below. The reddish powdery coating on the other side was probably produced during the excavation works. At the foot of Pantheon, the roof presents multiple interpenetrating rising cupolas forming a giant rising channel morphology, indicating flow rising from to NE, toward Pantheon that acted as a phreatic lift (Fig. 8H). The gallery of Pozzo dell'Ade develops along a fracture parallel to the one that guided the first 200 m of the cave. Pozzo dell'Ade is a large shaft, which bottom is not visible anymore, partly filled with tunnel construction debris. On the current bottom of Pozzo dell'Ade, a narrow fracture-guided passage continues to the E (Crystals Gallery III). This area is entirely covered with recent calcite and aragonite bushes and crystals; it has not been investigated to avoid the damage to the delicate speleothems. Observations of morphology and the original flow direction suggest Pozzo dell'Ade being the main source of upwelling of deep water and this shaft can thus be considered as a major feeder of the original cave system (Fig. 5C). Another fracture-controlled shaft is present 30 m further to the SW (Crystals Gallery II), also not investigated for conservation purpose. This might be another feeder. Except some small active epigene drippings, no other flow source has been detected.

The Crystals Gallery I develops after the artificial tunnel connecting to Bàsura Cave. Here, floor, walls, and roof are almost entirely covered with delicate bushes and needle crystals (Fig. 8I). Channelized flows of warm and moist air that condenses and partially corrodes the rock have carved condensation channels along the roof (Fig. 8I). When not covered with crystals coating, the host rock displays a deep weathered layer of soft red-brown material. Similar weathering material is also visible in places in the Gallery of Pozzo dell'Ade.

Fluvial deposits are visible only in a few places. In the entrance *Tanone* Gallery, a pebble deposit has been found below one of the old flowstones (TO22, Fig. 8B). Some quartzite gravels clearly show an external origin from fluvial material. In the excavated tunnel below Pantheon, a sand layer (TO16b), also containing quartzite gravels, shows a progradant structure toward Pantheon, which testifies to the ancient flow direction toward the NE (Fig. 8F). Finally, only fine clay sediments are present in the Crystals Gallery (T10, T11), mainly composed of detrital material (quartz, feldspar, muscovite/illite), and corresponding to the finer distal part of the coarse fluvial material identified before.

Several calcite deposits have been sampled here for U/Th dating (Tab. 2). The *Capitelli* testifies to the presence in the past of large pools where outgassing caused the slow deposition of mammillary calcite and shelfstones (Bontognali et al., 2016; De Waele et al., 2018). The stipe of the "mushrooms", because of their typical steep conical shape, is probably formed by up to 2 m-high raft cones, although none is broken, so they might also be common stalagmites.

The crystals covering Crystals Gallery and the weathered material of the inner confined area have been sampled for mineralogical analyses (Tab. 1). In addition to calcite bushes and aragonite needles (Fig. 8I), the white soft porous deposits are made of hydromagnesite, dolomite, and magnesite (T5, T6), and the pasty moonmilk (T9) of calcite. The weathered rock materials (T7, T8, TO12) show the presence of hematite, goethite, muscovite/illite, and quartz, together with a large amount of calcite and dolomite host rock particles (Tab. 1).

Finally, large bat colonies were present in the past in entrance gallery (Tanone), as indicated by discrete remnants of phosphate crusts in cupolas. The guano deposit probably disappeared because of mining of local inhabitants and from the considerable reworking of the floor for the tourist trails. However, due to the presence of a thick calcite plug between *Tanone* and *Capitelli*, bats were not able to access the inner part of the cave that remained strictly confined.

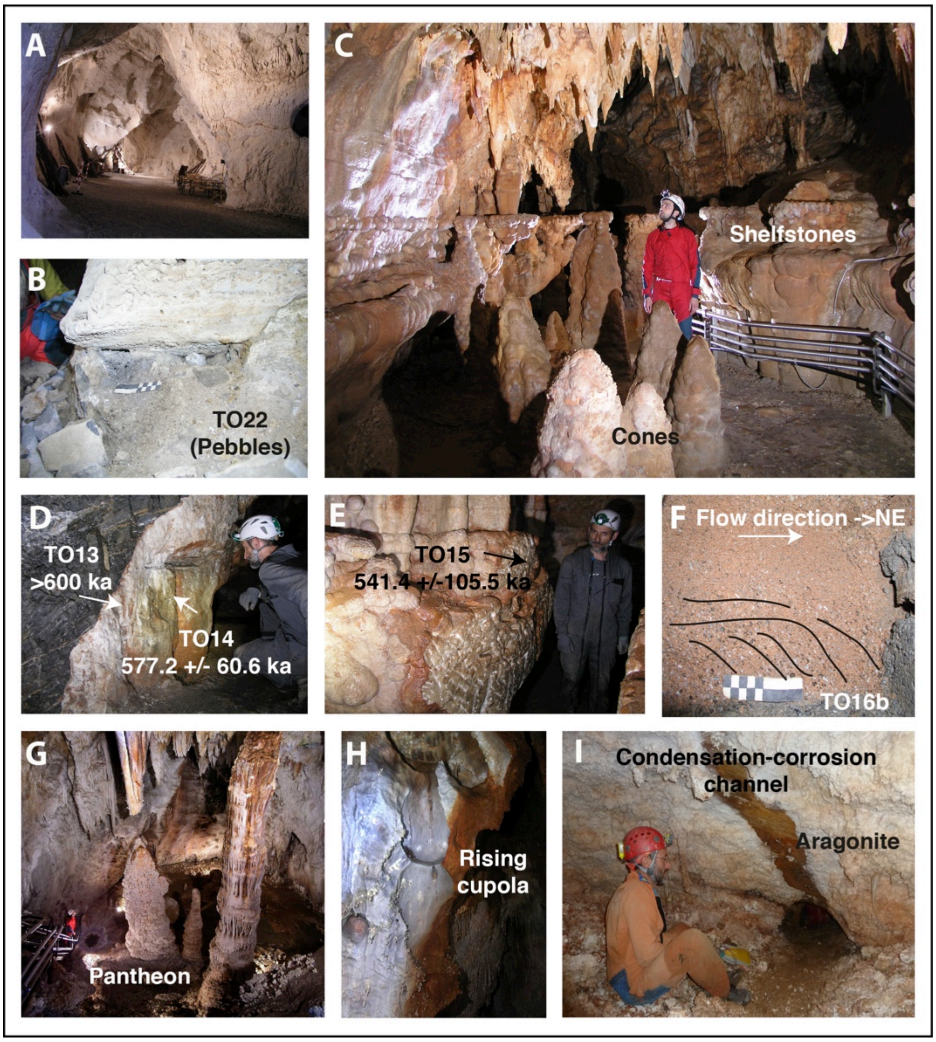

Fig. 8. Morphologies and deposits in Lower Santa Lucia Cave (Photos by Jean-Yves Bigot): A. The large Tanone gallery following the entrance displays walls with weathered rocky surfaces and very sparse remnants of corroded flowstones.; B. The fluvial pebble deposits (TO22) in Tanone gallery, not far from the entrance; C. Capitelli, with the raft cones in the foreground, and the different levels of shelfstones forming the mushroom-like speleothems; D. The end of the artificial tunnel shows dark dolomite with white veins (left), where white mammillary (subaqueous) calcite (TO13) is covered with a younger brownish calcite (TO14) representing a flowstone or shelfstone (subaerial); E. The top shelfstone of the mushroom-like speleothems (TO15), representing the youngest generation of TO14; F. Gravel deposit (TO16b) just below the Pantheon, underlying a dated flowstone level (TO16a); interpretation of progradation structure shows a palaeo-flow toward the NE; G. The nice Pantheon room, flow welled up from the hole below the person; H. The chain of

rising cupola between Pozzo dell'Ade and Pantheon also showing flow toward NE; I. The narrower passages in Crystals Gallery are entirely covered with aragonite and other white minerals, cut by a clear condensation-corrosion channel on the roof, where rock is deeply weathered (Photo by Philippe Audra).

4.1.4. Bàsura Cave

Bàsura Cave opens at an altitude of 186 m asl, with two neighbouring entrances less than 10 m apart (Fig. 5D). Shortly after the connection of both entrances, there is the passage opened in 1953. The horizontal passage gradually increases in size, then a large flowstone ascends toward the Footprints Corridor. Several narrow passages on the NE side give access to side branches descending to the lower parts of the cave (Fascio, Small Lakes). Proceeding inward, the passage is occupied by a lake, formed by recent infiltrating water, the only sign of temporary water flow in the cave. A large rimstone dam is broken and has blocked the transport of large cave bear bones. From here on, the floor of the cave is effectively a riverbed, and the related fluvial sediments are mainly composed of clay with numerous cave bear bones and skulls. Then, the cave becomes narrower and starts descending toward Cibele (Fig. 9B). In the lower segments, white subaqueous well-developed speleothems indicate that this section has been underwater for a rather long period of time (Fig. 9C). Before its recent draining, this part of the cave was still underwater. On the bottom of Cibele, the downward continuing branch is filled by blocks. An artificial 110 m-long tunnel connects Bàsura to Lower Santa Lucia Cave.

Regarding the type of flow at the origin of the cave, the narrow side branches (Fascio, Small Lakes) descending to lower sectors, show signs of rising flow. These lower passages are most probably ancient feeders of the original cave system (Fig. 5D). It is highly probable that the downward continuing branch at the base of Cibele was another feeder of the original system. The main passage shows rising features, cupolas, widened fractures, rock fins. All is compatible with very slow flowing water, completely lacking marks of turbulent flow such as scallops or allogenic coarse sediments.

Many signs of intense corrosion are visible throughout the main passage affecting walls, such as widened corroded fractures and condensation-corrosion pits. Speleothems also show very clear signs of corrosion especially in the vicinity of the side branches (Fascio, Small Lakes). Finally, both entrances have become perfectly circular as the result of condensation-corrosion (Fig. 9A).

Two types of sediments are present. Close to the entrances, the floor is covered with angular cryoclastic elements showing an infill from external slope material. These sediments disappear inward, leaving place only to fine sediments. Only one place shows fluvial sediments, at the start of the steep descent towards Cibele: a sandy-gravel quartzose deposit in a red-brown matrix has been sampled (TO17, Fig. 9D).

Speleothems cover extensive surfaces (Figs. 9B, 9D). In Cibele, the passage is entirely covered by subaqueous mammillary calcite, which was still actively depositing before the artificial draining in the 60s (Fig. 9C). Cibele also displays pool fingers (microbial filaments gradually thickened by subaqueous mammillary calcite coating), which are up to 5m-tall and 20 cm of diameter. Such dimensions are probably unique for Europe. In addition, calcite rafts, after sinking down, were coated by up to 1 cm-thick subaqueous calcite (Fig. 9E).

Many speleothems have been dated by U/Th in the past, to constrain the human frequentation, which is attested from at least 150 ka (Arobba et al, 2008) indicating that the cave was already connected with the surface at that time. Footprints were instead left by *Homo Sapiens* around 14 ka (Citton et al., 2017), attesting that the cave was still accessible. Indeed, the entrance flowstone that closed the cave after human incursion reported an age between 205±24 ka and 12.34±0.16 ka (Molleson et al., 1972). A large flowstone nearby the Footprints Corridor is certainly older than 615 ka. Indeed, the flowstone appears to have grown from the MIS13 (over 500 ka) to the beginning of MIS7 (around 240 ka) (Pozzi et al., 2019). In addition to these previous studies, we collected three calcite samples for U/Th dating (Tab. 2 and Fig. 9).

Three samples of calcite rafts have also been collected in Bàsura Cave for stable isotope analysis (Tab. 4, Fig. 5C): an active raft deposit in the lower parts of Fascio Branch (T2), and two thick rafts in the Cibele area, one on in the higher areas before descending (T4) and one in the lowest part (T3).

Finally, even if bats entered the cave before its artificial enlarging, guano deposits are not abundant. They possibly could be either covered by calcite or the size of colonies was limited by the narrow entrance. In a small alcove in the Fascio Branch, a brown crust has been sampled (TO21), corresponding to a bat guano by-product (F- or OH-apatite, with detrital contamination of quartz and mica).

Fig. 9. Morphologies and deposits in Bàsura Cave (Photos by Jean-Yves Bigot (A-D-F) and Philippe Audra (B-C-E)): A. The rounded entrance of Bàsura Cave and the inclined strata; B. The steep descent towards Cibele, cut through the thick flowstone; C. The subaqueous mammillary calcite deposits of Cibele; D. The brownish sandy-gravelly deposits (TO17) below white calcite (TO17); E. The thick calcite rafts on shelves in the massive pool fingers covered with mammillary calcite; F. Subaqueous rafts integrated in a calcite sequence, sampled at the base of the Cibele room (TO19).

4.2. Mineralogy

A wide array of minerals were identified by XRD and SEM analyses, and are reported in Tab. 1. They belong to the classes of carbonates, sulphates, phosphates, oxi-hydroxides, and silicates.

Carbonates are represented by calcite [$CaCO_3$], aragonite [$CaCO_3$], dolomite [$CaMg(CO_3)_2$], hydromagnesite [$Mg_5(CO_3)_4(OH)_2 \cdot 4\ H_2O$] and huntite [$Mg_3Ca(CO_3)_4$]. Pure calcite composes rafts in Bàsura and Colombo caves (samples T3, T4 and C2), as well as the pasty material (moonmilk) found in Lower Santa Lucia Cave (T9). Calcite and aragonite are the main components of weathering material originating from the disaggregation of the walls, as expected in caves developed in limestone and dolostone. It is often mixed with detrital material (T7, T8, T11, T12). In Crystals Gallery, warm airflow causes the development of Mg-rich minerals growing on aragonite frostwork, including huntite, and hydromagnesite, deriving from evaporation increasing the Mg/Ca ratio of percolation and moisture at the contact of the walls (T5, T6, T1).

Oxides are represented by hematite [Fe_2O_3] (TO9b, T8) and titanomagnetite [$Fe^{2}(Fe^{3+}, Ti)_2O_4$] (T7), and hydroxides by goethite [$FeO(OH)$] (TO12). They may originate either from fluvial or detrital material brought from the surface, or from weathering of detrital material through acidic bat guano, or from red clay veins inside the rock.

Finally, silicates are represented by quartz, feldspar, and phyllosilicates (illite/muscovite, clinochlore). They are present in fluvial deposits (TO6, TO10, T11, TO16b, TO22, TO17), mixed as dust with other deposits such as guano (TO9a, TO9b) or phosphate deposits (TO11, TO21), or as constituent of weathered material associated with host rock particles (T8, TO12).

Table 1. Mineralogy of samples taken in the different caves (C = Colombo; LSL = Lower Santa Lucia; B = Bàsura). Hm = Hydromagnesite; Hu = Huntite; Ar = Aragonite; Ca = Calcite; Do = Dolomite; Gy = Gypsum; Br = Brushite; Ard = Ardealite; Nb = Newberyite; Le = Leucophosphite;

Sp = Sphenisciddite; Ap = Fluorapatite or Hydroxylapatite; Q = Quartz; He = Hematite; Go = Goethite; Ma = Ti-magnetite; Il = Illite; Mu = Muscovite; Fs = Feldspar; Cl = Clinochlore

ID	Cave	Sampling site	Observations	Minerals
C1	C	Main room	Hard yellow crystals on guano	Gy, Nb
C2	C	New branch after gate	Recent calcite rafts	Ca
C3	C	Main room	Yellow soft material on guano	Ard, Br
TO6	C	Ceiling pocket at entrance of chamber	Cemented sand, younger than TO5	Detrital (Q, Mu)
TO9a	C	Main Chamber, inner wall	Yellow gypsum flower	Gy, Le + detrital (Q, Mu/Il)
TO9b	C	Main Chamber, inner wall	Beige phosphate deposit, drier than where gypsum is found	Gy, Le, He + detrital (Q, Mu/Il, Fs)
TO11	C	Side passage before chamber	Dark phosphate crust	Ap, Ca + detrital (Q, Mu/Il, Fs)
T5	LSL	Crystals Gallery	White deposit on floor	Hm, Do
T6	LSL	Crystals Gallery	White deposit on crystals on the wall	Hu, Hm, Do
T7	LSL	Crystals Gallery	Weathered wall with boxwork	Ca, Ma
T8	LSL	Crystals Gallery	Brick red weathering material	Ca + detrital (Q, Il, Cl), He
T9	LSL	Crystals Gallery	Yellowish pasty material	Ca
T10	LSL	Crystals Gallery	Residual fluvial green-grey clay in fracture	Detrital (Q, Mu)
T11	LSL	Crystals Gallery	Fluvial sediment	Do + detrital (Q, Mu, Cl)
TO12	LSL	Above Pozzo del Ade	Weathered wall	Ca (75%) + detrital (Mu/Il, Fs), Go
TO16b	LSL	Gallery below Pantheon	Progradant sandy deposit below calcite (TO16a)	Rounded detrital elements (Q, quartzite, He/Go, Fs)
TO22	LSL	Tanone	Several samples of pebbles below old stalagmite	Rounded detrital elements (Q, quartzite, He/Go, Fs) in Ca cement
T1	B	Fascio, lower parts	White dots on the wall	Hm, Hu, Ar
T3	B	Base Cibele	Old thin stratified calcite rafts	Ca
T4	B	Top of Cibele, first room	Thick calcite rafts	Ca
TO17	B	Slope down to Cibele	Sand below white calcite (TO18)	Rounded detrital elements (Q, quartzite, He/Go, Fs)
TO21	B	Fascio, small inlet in entrance series	Brown phosphate crust	Ap + detrital (Q, Mu/Il)

4.3. Geochronology

A summary of the obtained U-Th ages is reported in Tab. 2, which comprises the sampling locations and field observations. The full U-Th dataset is instead provided in Supplementary Tab. 1. ^{238}U content of the dated samples spans between 1719.3 and 81.2 ppb (average: 400.7 ppb). With the exception of TO5 sample, detrital ^{232}Th contamination is low. The latter is expressed by the $^{230/232}$Th activity ratio (Sup. Tab. 1), with higher ratios indicating low contamination and *vice versa*. This guarantees that the resulting ± 2σ uncertainty is relatively low. The U-Th radiochronology allows to attain ages back to 550-600 ka (Hellstrom, 2003); ages around this limit can report relatively high uncertainties, because of the inaccuracies in measuring the very low content of residual uranium. Ages beyond this limit cannot be constrained, and are reported as >600 ka. In Toirano karst system, the dated samples span between 35.1 ± 0.3 ka obtained from mammillary calcite in Bàsura Cave (sample TO20) to >600 ka for several samples (TO5, TO10, TO13, and TO18) from Colombo, Upper Santa Lucia and Bàsura Caves (Tab. 2 and Sup. Tab. 1). Several speleothems resulted older than 500 ka, in Lower Santa Lucia (TO14, TO15 and TO16) as well as in Bàsura (TO19). The remaining samples are comprised between 179.7 ± 4.1 (TO8, Colombo Cave) and 407.6 ±22 ka (TO3, Upper Santa Lucia Cave), with TO4 and TO7 reporting intermediate ages respectively at 343.0 ± 10.4 and 375.5 ± 14.8 ka.

Cosmogenic dating reported an age of 1.798 Ma (Tab. 3), with ^{10}Be concentration at the upper limit. The latter impeded a reliable calculation of the relative uncertainty. Despite this limitation, and the non-replicated data, we believe this age is reliable enough considering the well-established applied methodology as well at the stratigraphic agreement with the ages obtained by U-Th dating.

Table 2. U-Th ages and relative 2σ uncertainties. Ages older than the limit of the U-Th method are reported as >600 ka. Caves: C = Colombo; USL = Upper Santa Lucia; LSL = Lower Santa Lucia; B = Bàsura. See Suppl. Tab. 1 for the complete U-Th dataset.

ID	**Cave**	**Age (ka)** ± 2σ	**Sampling site**	**Observations**
TO5	C	>600	Entrance Central Room	Calcite layer older than TO6
TO7	C	375.5 ±14.8	Entrance Central Room	Corroded flowstone
TO8	C	179.7 ±4.1	Central Room	Old corroded calcite in pocket
TO10	C	>600	Lateral branch of Central Room	Old white calcite floor
TO3	USL	407.6 ±22	After station 10	Old stalagmite
TO4	USL	343.0 ±10.4	After station 10	Border of less old rimstone dam
TO13	LSL	>600	Entrance *Capitelli*	Subaqueous calcite older than TO14
TO14	LSL	577.2 ±60.6	Entrance *Capitelli*	Pool calcite, younger than TO13

TO15	LSL	541.4 ±105.5	Entrance *Capitelli*	Upper part of *Capitello*
TO16	LSL	581.3 ±143.3	Passage below Pantheon	Calcite layer on sands
TO18	B	>600	Down to Cibele	White calcite covering sands of TO17
TO19	B	562.3 ± 77.1	Bottom Cibele before tunnel	Old subaqueous calcite in Cibele
TO20	B	35.1 ± 0.3	Small Lakes	Mammillary calcite

Table 3. Cosmogenic burial age of quartz gravels in Colombo Cave (C). (*) = due to ^{10}Be concentration at the upper limit, uncertainty could not be calculated, ASTER, 5MV AMS facility.

ID	**Cave**	**Sampling site**	**^{10}Be (at/g)**	**^{26}Al (at/g)**	**Burial age (Ma)**
TO	C	Inner wall of central room	8 453*	24 621 ± 15 053	1.798

4.4. Stable isotopes and temperature estimates

Stable isotopes of the selected samples range between -4.4‰ to -5.9‰ VPDB and -8.24‰ and -10.02‰ VPDB in $\delta^{18}O_{calcite}$ and $\delta^{13}C_{calcite}$, respectively (Tab. 4). Regarding $\delta^{18}O$-derived temperature, estimates are represented in Tab. 4 using the range of obtained $\delta^{18}O_{calcite}$ and the mean value (-5.2‰ VPDB), in relation to the modern $\delta^{18}O_{water}$ (-5.8 ± 0.5 ‰ V-SMOW). Uncertainties in the latter limit the calculation of precise paleo-temperatures, so the results are here presented as a broad estimate by using the symbol "~". The estimated uncertainties for the palaeo-temperatures is around ±3 °C. Our calculations suggest that water temperature has never exceeded ~23 °C (when using values of -5.3‰ and -4.4‰ for $\delta^{18}O_{water}$ and $\delta^{18}O_{calcite}$, respectively) and was not lower than ~10 °C (when using values of -6.3‰ and -5.9‰ for $\delta^{18}O_{water}$ and $\delta^{18}O_{calcite}$, respectively), during the precipitation of calcite speleothems in the Toirano caves.

Table 4. Speleothem calcite stable isotopes ($\delta^{18}O_c$ and $\delta^{13}C_c$) and estimated palaeo-temperatures (local $\delta^{18}O_w$ = -5.8 ‰, from Cavallo, 1990). C = Colombo; B = Bàsura.

ID	**Cave**	**Location**	**$\delta^{18}O_c$**	**$\delta^{13}C_c$**	**Modern $\delta^{18}O_w$**	**T (°C) estimate**	**T uncertainty estimate (°C)**
C2	C	Old calcite raft	-5.90	-8.24	-5.8	~20	~ ±3
T2	B	Active calcite raft	-5.37	-10.02	-5.8	~17	~ ±3
T3	B	Calcite raft, lower part of Cibele	-4.98	-9.66	-5.8	~15	~ ±3

T4	B	Calcite raft, upper part of Cibele	-5.70	-10.65	-5.8	~19	~ ±3
TO18	B	Old flowstone (>600 ka), Upper Cibele	-5.12	-8.17	-5.8	~16	~ ±3
TO19	B	Old flowstone (562 ka), Lower Cibele	-5.24	-9.32	-5.8	~17	~ ±3
TO20	B	Recent mammalies (35 ka), Lakes	-4.40	-9.09	-5.8	~12	~ ±3

Transmitted-light microscopy has revealed the presence of primary monophase fluid inclusions in sample TO19 (Fig. 10). The inclusions show characteristic inverted edges, indicating their primary origin. Primary monophase fluid inclusions either appear isolated (Fig. 10A) or are clustered in fluid inclusion assemblages (Fig. 10B). No primary two-phase fluid inclusions were observed in this sample. The occurrence of only monophase liquid inclusions imply that mineral crystallisation occurred in a low-temperature (ambient-like) thermal environment, certainly less than ~50 ˚C.

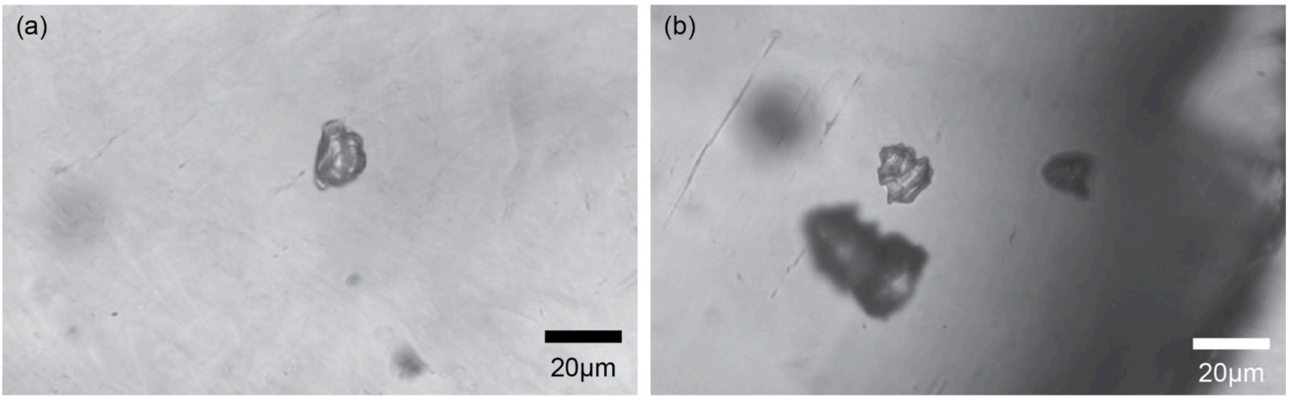

Fig. 10. Examples of primary all-liquid fluid inclusions in TO19 calcite (a, b). Fluid inclusions show characteristic inverted growth steps (b). Photomicrographs are the courtesy of Yves Krüger.

5. Discussion: speleogenesis of Toirano karst system

5.1 Morphological indicators of speleogenesis

Although the original shape of the caves and their meso-morphologies have been greatly modified by later processes, several morphological observations in the different caves have shown a series of important speleogenetic indicators:

1. The different remnants of the cave system are developed along clearly distinguishable levels, at altitudes of 340 (Ulivo), 250 (Colombo), 215 (Upper Santa Lucia), 210-205-200 (Lower Santa Lucia), and 185-175-165 m asl (Bàsura), respectively (Fig. 11). These subhorizontal cave passages are clearly recognisable in the four upper caves, and are less clear only in Bàsura Cave, albeit still distinguishable and comparable with cave passages at similar altitudes in Lower Santa Lucia Cave (Fig. 11). These cave levels do not appear to have been influenced by local structural features (i.e.strata are tilted), and their very low inclination (close to horizontal) can best be explained by their evolution close to the former water table. These cave levels testify to relative long-lasting stable phases in which the local base level and caves were at the same altitude.

2. Morphologies suggesting fast and turbulent flow (scallops) have not been detected. Clastic sediments range from gravel to clay. Apart from angular clasts located in entrance areas (especially Bàsura), which have been brought in by gravity or by solifluxion, the largest elements (pebbles) are located close to entrances with inward grain size decrease, clearly pointing toward intrusions of allogenic fluvial material. This is also evidenced by their petrographic composition (quartzite, schist), which agrees with the source areas located nearby the Toirano area (Fig. 2). Cave passages have been entirely filled by these sediments, at least for the first 100-200 m from the entrances. In the inner parts of the system, only smaller grain sizes are visible (gravels, sands), as long as they are not concealed by later speleothem deposition. Samples TO16 and TO17 show a reworking of the allogenic material by internal flow toward outlets that maintained their activity during the infilling periods. Finally, fine sediments derive from a mixing of different sources, i.e. carbonates grains from disaggregation of the host rock, clays and iron oxides from insoluble material and red clay veins, and from allogenic fluvial sediments, as evidenced by typical minerals (quartz, mica, feldspars) trapped in the weathered material along the walls.

3. The caves are characterised by morphologies suggesting slowly flowing waters, and it is clear from observations in several cave areas that these fluids followed ascending paths. These morphologies are rising channels, superposed cupolas and ceiling channels. Some ascending

conduits are almost certainly ancient feeders. Except from limited seepage spots, no trace of significant epigene recharge, either active or inactive, such as vadose shafts and meanders, have been detected. The hydrological circulation at the origin of the cave system is clearly hypogene (*sensu* Klimchouk, 2007), implying upward recharge from a deep route, with surface water minimally influencing flow discharge and the chemico-physical characteristics of the fluids. Several morphologies detected in the Toirano karst system are similar to a recent case study where phases of hypogenic speleogenesis have been well documented (Pérez-Mejías et al., 2019).

4. Condensation-corrosion, both by convection of external warm and wet air masses, and vapours produced by bats and decay of guano deposits, have intensely modified walls and roof morphologies in many portions of the caves, especially in the higher parts of the system that were not confined (Colombo, Upper and Lower Santa Lucia caves). This has made it difficult to recognise many of the typical morphologies of rising flow.

5. The active thermal and slightly sulphidic spring in the village of Toirano, less than 700 m south of the caves and ~100 m below the Bàsura Cave, indicates ongoing processes of deep fluid circulation today. Analogously, deep fluid circulation might have been active in the past; hypogene fluids circulating in the carbonate rocks would have caused the formation of the karst network.

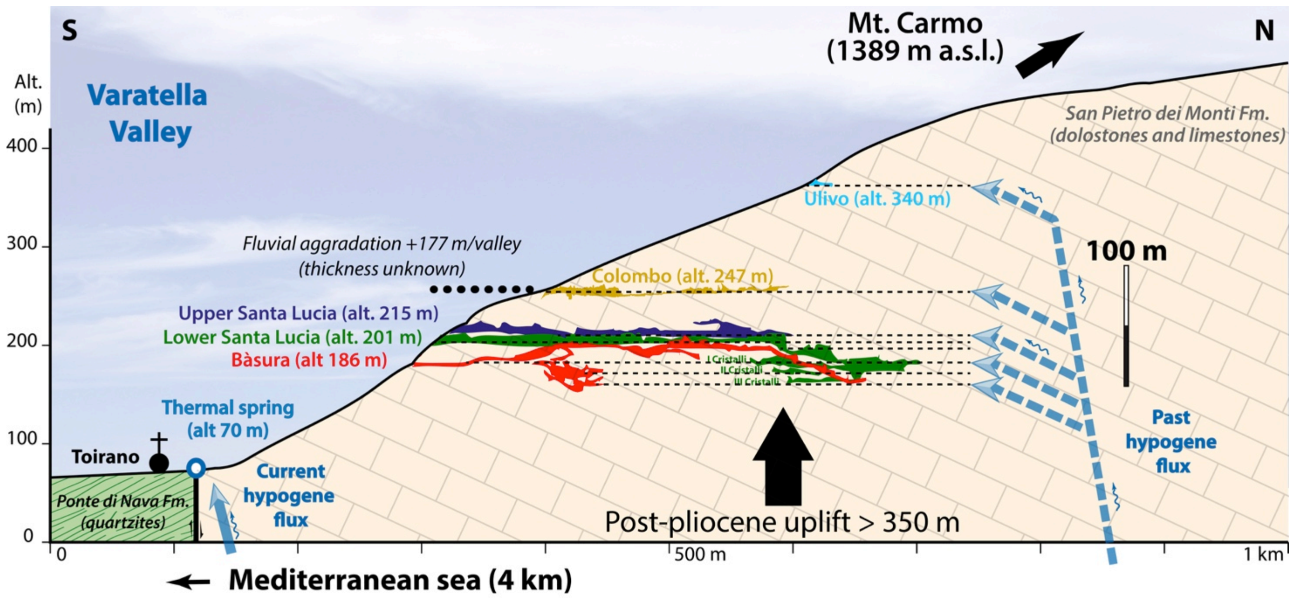

Fig. 11. Schematic profile through Mt. Carmo showing the altitudinal distribution of the cave levels in relationship to their hypogene origin, the uplifting and correlated Varatella valley deepening (Surveys courtesy of Gruppo Speleologico Cycnus and Delegazione Speleologica Ligure, 2001).

5.2. Hypogene origin of the system

The mineralogical analyses did not evidence the typical weathering by-products of sulphuric acid speleogenesis such as alunite and jarosite (D'Angeli et al., 2018). In addition, there are no massive gypsum deposits, and the observed tiny gypsum minerals were always associated to guano deposits. Instead, carbonate minerals abound, including calcite, aragonite, huntite, and magnesite (minerals typically found in dolostone-hosted caves), whereas gypsum, ardealite, brushite, F- and OH-apatite, leucophosphite/spheniscidite, and newberyite have been found on the old guano deposits (Audra et al., 2019, Tab. 2).

The caves formed within the carbonate rock mass without a direct connection to the surface, and before the Varatella torrent started carving its deep valley. Possibly thermal fluids rose along deep-rooted sub-vertical faults concentrating their corrosive action close to the water table, where the dissolved CO_2 was able to escape into the above lying air-filled chambers. Most dissolution occurred close to the water-air interface, and in the aerate part of the caves because of condensation-corrosion. The action of minor amounts of H_2S-enriched fluids cannot be entirely excluded, based on the sulphide amount of the spring still active today (25.4-37.0 mg L^{-1}; Calandri, 2001), although clear evidences of sulphuric acid speleogenesis (SAS) have not been found. However, the signs of sulphuric acid interaction with the host rock, both weathering products (gypsum and other sulphates) and typical corrosion morphologies (e.g., replacement pockets), could have been easily weathered by the intense and long-lasting condensation-corrosion processes, and/or covered by the recent action of infiltration waters and speleothem deposition. It is more likely that the cave-forming fluids were rich in CO_2, and might have been slightly thermal, whereas sulphate (and sulphuric acid) played only a minor role (if at all). Accordingly, we claim that the

Toirano caves are of hypogene origin, with the earliest speleogenesis governed by the upwelling of possibly low thermal fluids rich in CO_2.

Stable isotope analyses, however, have pointed to palaeo-temperatures ranging from ~12 ± 3 to ~20 ± 3°C (Tab. 4). Considering uncertainties, temperature estimates never exceed ~23°C and were never lower than ~10°C. Such values span between the current temperature found at the active thermal spring of Toirano (22-23°C) and the present climate in the valley (Toirano city 14.3°C). This variability could be related to the different climate periods during which calcite deposited. Accordingly, recent (35 ka) mammillary calcite of "Small Lakes" (T20), deposited during the last glaciation, reported the lowest estimate (12 ± 3 °C, Tab. 4). Active rafts reveal a temperature of ~17°C, which is close to the current cave temperature and mean annual average, and lower than the thermal spring temperature. Ancient flowstones (TO18-19) and rafts (T3-4) show a temperature range between ~15 and ~19 °C (Tab. 4), likely driven by palaeoclimate changes as quoted above. The presence of all-liquid primary fluid inclusions in one of the calcite rafts from the Cibele area also suggests that the mineral depositing fluids were characterised by temperatures lower than ~50°C (non-hydrothermal) (Fig. 10). We suggest that all cave calcite deposited from infiltrating waters, at times mixing with slightly thermal water. The calcite $\delta^{13}C$ values (between -8 and -11‰, Tab. 4) are consistent with a contribution from above lying soils rather than a pure hypogene flux (McDermott, 2004). This is confirmed also by the $\delta^{18}O$ values, which are typical of low temperature calcites precipitating from mid-latitude rainfall waters (Columbu et al., 2018). The fact that the last glacial T20 sample reported the lowest temperature supports that infiltrating water had a primary role in speleothem precipitation.

Most of the calcite speleothems visually appearing as very old deposits reported ages beyond the U-Th method limit (ca. 600,000 years), even in the lower (and possibly youngest) caves (Tab. 2). The age of underground deposits can be used to constrain the minimal age of the cave (Columbu et al., 2015; 2017). Consequently, the entire karst system and even the lower cave levels are certainly older than 600 ka. Similar results were obtained by Bahain (1993), with the base of a flowstone in

Bàsura Cave showing reverse magnetic polarity (thus certainly older than 780 ka); ESR dates of faunal remains in this basal sequence reported ages between 502 (±47) and 748 ka (±66), whilst several U/Th dates resulted older than 557 ka (Shen, 1985). This is also confirmed by recent studies in Bàsura Cave, where the bottom of a 2 m-thick flowstone resulted older than 615 ka (Pozzi et al., 2019).

The allogenic sands sampled in Colombo Cave have delivered a burial age of approximately 1.8 million years, which represents the minimum possible age of the voids filled by these sands. These coarse-to-fine sands have been carried into the caves during the Lower Pleistocene high stands, by rivers that aggraded their thalwegs because of the rising sea level. During the Gelasian (ca. 2.6-1.8 Ma) the sea level, which greatly controlled the base level for the studied caves, oscillated globally between -100 and +10 m with respect to present sea level (Rohling et al., 2014). By considering the ~1.8 Ma age in Colombo, and the elevation of the cave over the Varatella valley (~180 m), the resulting incision rate can be estimated at 0.1 mm y^{-1}. The incision of the Varatella valley possibly responded to the uplift of the area north of the main fault (on which the thermal spring is located). This rate is slightly overestimated (Colombo Cave is older than 1.8 Ma, so the real incision rate is lower), since the cave formed before the intrusion of the dated sands (possibly at the Upper Pliocene/Lower Pleistocene). However, this value is in agreement with the long-term uplift rates estimated in a coastal area 20 km East of Toirano (e.g., 0.086-0.20 mm y^{-1} in Carobene and Cevasco, 2011; 0.08-0.16 mm y^{-1} in Carobene and Firpo, 2002). Taking into account the estimation of the incision rate of the Varatella valley (0.1 mm y^{-1}), we can tentatively estimate the age of all cave levels: Ulivo Cave might have an age of ~2.7 Ma, Colombo Cave would have formed around 1.8 Ma (given the cosmogenic dating), Upper Santa Lucia Cave 1.5 Ma, Lower Santa Lucia 1.3 Ma, and Bàsura Cave around 1.2 Ma (Tab. 5).. According with our estimates, the speleogenesis of the Toirano cave system occurred during the Gelasian and Lower Calabrian, and probably at the very end of Pliocene for the highest Ulivo Cave. The presence of a Messinian canyon offshore, and Pliocene Gilbert-delta deposits onshore in the vicinity of the current coastline, evidence that the valley significantly entrenched during the Messinian Deep-sea-level, then was refilled during the Pliocene by sediments sourced from the ongoing uplifted mountain where strong erosion occurred. The discontinuous uplift of the study area mainly took place during the Upper Pliocene - Lower Pleistocene, with marine Lower Pliocene sediments now located at altitudes of up to 400 m asl (Carobene and Firpo, 2002; Ferraris et al., 2012). Then, following the Pleistocene uplift, a gradual entrenchment of the Varatella gorge occurred, with the removal of most of the Pliocene marine deposits and Pleistocene terraces. The old fluvial material, located above 100 m asl, has only been preserved in Toirano caves as intrusion material. They are possibly related to 1) aggradation or fluvial intrusion during Pleistocene, or 2) re-incision and injection in caves of the reworked material. The cosmogenic burial age at about 1.8 Ma, if reliable, would point toward the second option. Note that Colombo Cave predates this age, without indications on how much older this cave could be with respect to the sediment intrusion. Regarding ages obtained from speleothem U/Th dating, most are older than the method's limit (600 ka), making it difficult to ascribe an age to the subaqueous deposits related to the initial phreatic stage. However, the partial draining of the main pool stages (Capitelli in Lower Santa Lucia and Cibele in Bàsura, which are located at the same elevation), probably still fed by minor hypogene recharge, is quite well bracketed around 581-541 ka. Considering the age errors, this would correspond to a period between ca. 720 and 440 ka (Tab. 2 and 5). The pool-stage record in the well-marked shelves of Upper Santa Lucia is more recent (343 ±10 ka), even if the cave is located slightly higher. This would indicate that portions of the main cave levels (USL-LSL-B, see Tab. 2 for codes) were underwater for approximately 400,000 years, comprised approximately between 720 and 330 ka. The age of dated stalagmites, which could have developed during or after this active hypogene pool stage, confirms the partial or complete draining as early as 400 ka. Flowstones older than 500 to 780 ka in Bàsura (Shen, 1985; Bahain 1993, Pozzi et al., 2019) suggest that some parts of the cave system were drained earlier.

Table 5 - Estimated ages of successive evolution of cave levels

Cave	Alt. (m)	Proposed age of phreatic hypogene speleogenesis (Ma)	Age pool speleothems and flowstones (ka)	Age stalagmites (ka)
Ulivo	337	~2.7		
Colombo	247	~1.8	> 600	376, 180
Upper Santa Lucia	215	~1.5	343	408
Lower Santa Lucia	201	~1.3	581-541	
Bàsura	186	~1.2	562 - 35	
Thermal spring	70	Active		

5.3 Overprinting of late stage condensation-corrosion

5.3.1 Condensation-corrosion in the inner semi-confined parts of the cave system

Intense signs of condensation-corrosion are visible in the inner parts of the caves that were almost entirely confined before the artificial opening of the tunnel and calcite plugs, such as in the inner branches of Colombo Cave, in the (past) confined part of Lower Santa Lucia Cave, and especially in the Crystals Galleries. Here, walls are covered by boxwork and deeply weathered soft material in between, with red-brown or greenish coloured surfaces (Fig. 12A), whereas the dolomite host rock was originally black (Fig. 8D). The weathered soft layer is several centimetres thick. It is mainly composed of loose carbonate grains with a high porosity (>25-30%), with minor amounts of iron oxyhydroxides (hematite, goethite, Ti-magnetite) at the origin of the typical colour, and detrital minerals (quartz, mica, feldspars, illite). Carbonates are provided by the disaggregation of the host rock, detrital minerals are remnants of old sediment filling of fluvial origin brought from external sources, and iron oxyhydroxides originated either from host rock veins of red clay, or from the weathering of the detrital minerals.

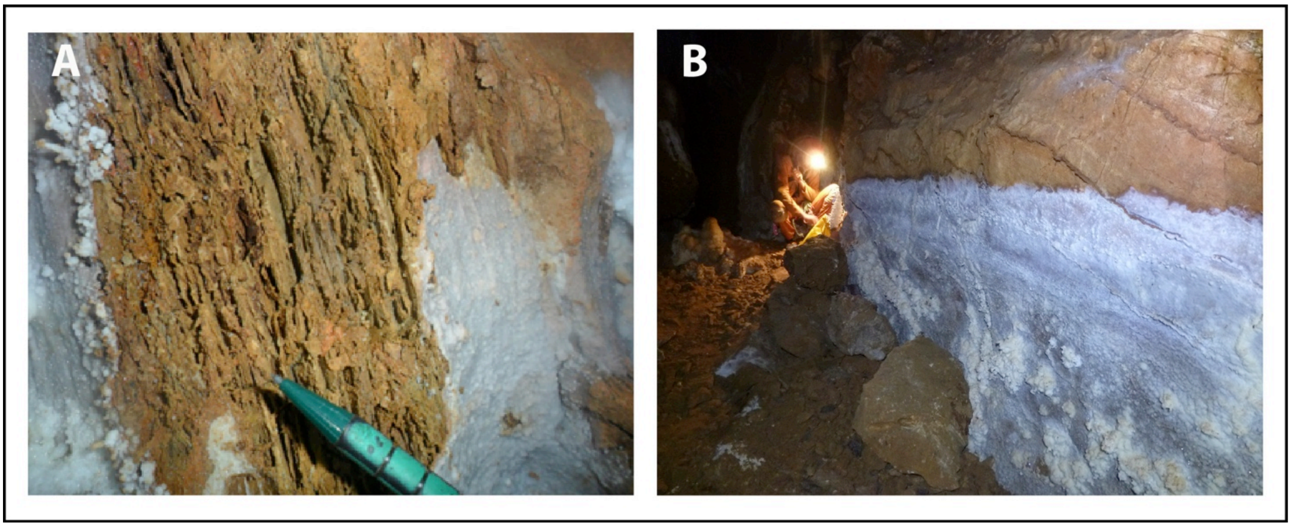

Fig. 12. Condensation-corrosion evidences: A. The black dolomite rock is deeply weathered by condensation-corrosion, making boxwork and soft residual material. Note the coating of evaporite minerals (calcite, aragonite, huntite, and hydromagnesite) (Photo by Jo De Waele); B. Air mass stratification in Crystals Gallery produces a sharp limit between areas of evaporation-precipitation downward and condensation-corrosion in the upper parts (Photo by Philippe Audra).

Many places in these confined parts are covered by a secondary carbonate coating, composed of minerals that are typically found in caves hosted in dolostone (calcite, aragonite, huntite, and hydromagnesite). This coating is present in the lower parts of the passages (lower walls and floor), whereas the upper parts generally display boxwork and weathered layers (Fig. 12B). Both are closely associated. In cave atmosphere close to moisture saturation, subtle air convections allow air mass stratification and exchange; condensation of higher warm moisture occurs on the cooler ceiling, whilst evaporation occurs in the lower parts of the passages in cooler and drier airflow. Condensation produces corrosion on the ceiling and a weathered layer, whereas evaporation produces crystallisation in the lower parts. The solutes produced by condensation-corrosion in the higher part of the passages descend by gravity across the weathered layer on top toward areas of evaporation at the bottom, where mineral precipitation can occur. The subtle airflow, currently present in the Crystals Gallery, which is directed toward the external cliff, clearly shows a still active process. Here a recent corrosion channel carves the white speleothem coating and the bedrock along the roof of the passage (Fig. 8I). However, such slow process requires long time to produce such deeply weathered layers. It possibly started after the early stages when hypogene caves began draining, but when slightly thermal water was still present at depth, or at least when the rock mass was still heated by the thermal fluids, producing rising warm and moist air flows. These processes clearly postdate the initial phreatic hypogene stage, which would have washed away the soft weathered material. Since many speleothems are older than 600 ka (Tab. 2) and some even older than 780 ka, one can expect that the condensation-corrosion process in confined cave areas occurred from about at least 1 Ma. The successive openings to the surface of some entrance parts drastically changed these semi-confined conditions, starting much more active condensation-corrosion processes boosted by active air circulation between the external atmosphere and the inner cave portions.

5.3.2. Condensation-corrosion and biocorrosion in the large entrance parts

Condensation-corrosion is particularly evident in the large passages of Colombo, Upper and Lower Santa Lucia, and in Bàsura caves. Importantly, the caves are located on a southwest facing cliff, where warm and wet air masses from the sea frequently rise along the valley and cause the formation of coastal fogs. During summers, the air masses coming from the sea have average temperatures well above 20°C, able to produce condensation on the cave walls that are around 15°C, or even colder. Furthermore, efficient air circulation prevents the cave atmosphere to warm up because of the release of condensation latent heat, keeping the cave walls colder than the entering air, and thus sustaining a continuous production of condensation waters. In the lower parts of the cave passages, dripping condensation waters, containing dissolved carbonates, fall to the ground and evaporate, causing the deposition of new microcrystalline calcite that is mostly removed by airflow. The highly undersaturated condensation waters have produced the weathering (partial dissolution) of the rock walls causing their powdery appearance.

In Lower Santa Lucia, the entrance passage (Tanone) is intensely corroded by condensation, mainly due to its large entrance allowing warm moist air circulation. Most of the flowstones have disappeared, except in sheltered corners (Fig. 8B). Here, remnants of coarse pebbles cemented by an old flowstone show that the passage has been entirely cleaned from its fluvial filling. It now displays as a large rounded conduit, with smooth wavy walls and a light colour due to the thin dry weathering layer (Fig. 8A). Compared to the passage size beyond the calcite plug isolating the Capitelli from Tanone, it clearly appears that Tanone conduit significantly expanded by condensation-corrosion, probably for several metres, cancelling most of its original features and sediments.

In Bàsura Cave, condensation-corrosion morphologies are also clearly visible: i) at the entrances, where the initially elliptical phreatic conduits have been subsequently rounded (Fig. 9A); ii) immediately behind the small passage that was opened in 1953; iii) on walls and speleothems intensely corroded by airflow. Here condensation is possibly related to the variations in pressure of the airflow, when the passage was still closed, and airflow experienced important pressure variations. This is confirmed by the fact that the signs of corrosion are most evident in the first ten metres from the (originally) narrow passage. In the Footprints Corridor, several speleothems are deeply corroded by airflows. Here, condensation is probably caused by the formation of a mixing cloud (Badino, 2010), since air convection from lower branches (Fascio, Small Lakes) mixes with air masses in this part of the cave. In addition, widened corroded fractures and condensation-corrosion pits, which are strongly developed, testify the intense activity of the process in this area.

The condensation-corrosion process is also boosted by bat colonies, which abundant presence in the past, considering the larger colonies and higher variety of species is testified by the large old guano and phosphate deposits. Phosphate forms crusts on carbonate walls and calcite speleothems mainly composed of F- and OH-apatite, whereas leucophosphite/spheniscidite form in presence of clastic material. More recent and still decaying guano is covered by sulphates and phosphates such as gypsum, ardealite, brushite, and newberyite (Tab. 1; Audra et al., 2019). Guano decay is an exothermic process releasing both water vapour and carbon dioxide, thus enhancing condensation above the guano heaps, and causing high CO_2 levels in the air. Other acids released by guano decay make the atmosphere particularly aggressive and corrosive. In addition, bat exhalations add other considerable amounts of heat, vapour, and carbon dioxide. All these aggressive solutions combine and are responsible of the biocorrosion of cave floor, walls, and ceiling, where cupolas are the most expressive features (Lundberg and McFarlane, 2009, 2012, 2015; Audra et al., 2016; Dandurand et al., 2019).

This powerful process can explain the exceptionally wide central room in Colombo Cave, where a central biconcave rock pillar is the leftover of intense expansion of original passages by condensation-corrosion (Fig. 6F). The same is testified by the presence of old corroded flowstones, as well as typical morphologies such as cupolas and the wavy (mega-cusped) appearance of the cave walls. Additionally, the pebbles that were introduced into the cave, and that probably entirely filled it, have completely disappeared, leaving only some patches of planed conglomerates in sheltered niches. Last but not least, the scarcity of graffiti (i.e. visitors' signatures) remnants shows the ongoing activity of corrosion processes. Based on our observations, the wall retreat by biocorrosion processes alone can here be estimated in at least 1 m on both sides of the passage, probably double on the roof.

In Upper Santa Lucia Cave, masses of old guano are still visible. Biocorrosion features are intensely developed. Interpenetrating cupolas are carving the chamber ceilings, cutting both rock and old calcite speleothems (Fig. 7D). Dripping pots are developing on the vertical of ceiling pendants that concentrate condensation runoff (Fig. 7E). However, on the contrary to Colombo Cave, actual biocorrosion processes seem to be subdued, as testified by the considerable amount of well-preserved graffiti, even on top of cupolas that are the places of the most intense condensation. This could be explained by the continuous frequentation of the cave by pilgrims and by the gating of the inner part (Fig. 7A) that prevented intrusion of bats for centuries, and thus preserved the historical traces of frequentation.

6. Conclusions

On the basis of the geomorphological observations, supported by geochemical analyses and radiometric dating, the origin of these complex caves cannot be attributed to a "classical" epigene vadose and phreatic speleogenetic model only. The Bàsura-Santa Lucia-Colombo caves formed by the action of rising hypogenic fluids that followed deep-rooted subvertical fractures. The rising conduits (*feeders*) are still visible in the lower levels of the cave system (Bàsura and Lower Santa Lucia caves), whereas they are obliterated in the higher and older levels by abundant authigenic and residual sediments. In the lower passages, the traces of ascending fluids are still well visible in many areas, with rising channels and superimposed cupolas.

Based on the observations made in the highest of the studied caves (Colombo) the following speleogenetic scheme can be presented (Fig. 13): A) The cave started forming at the water-table level fed by a deep-rooted fracture, with slightly thermal (possibly H_2S-rich) waters carving the cave in both phreatic, but mainly aerate conditions; B) A marine transgression during the final phases of the Pliocene and Early Pleistocene caused the river valleys to aggrade and enlarge; the entrance of the cave was completely filled with gravels and sands (pockets on the roof of the cave are still filled with remnants of these sediments, which burial age is around 1.8 Ma); C) successive Pleistocene uplift phases of the mountains caused the Varatella torrent to entrench, partially emptying the cave which, at least in the early stages, was probably still actively enlarging by rising hypogene fluids. The continuous uplift caused the intersection of the water table with the feeding fractures to shift laterally and to lower elevations, causing the formation of the lower levels of the cave system; D) in the final stages the cave system was abandoned by flowing hypogenic waters, and since then the large cave entrances are affected by air circulation, bat roosting and frequentation. Condensation-corrosion processes started to remove most remnants of the older sediments and speleothems (several of which are beyond the U/Th dating limit, i.e. > 600 ka).

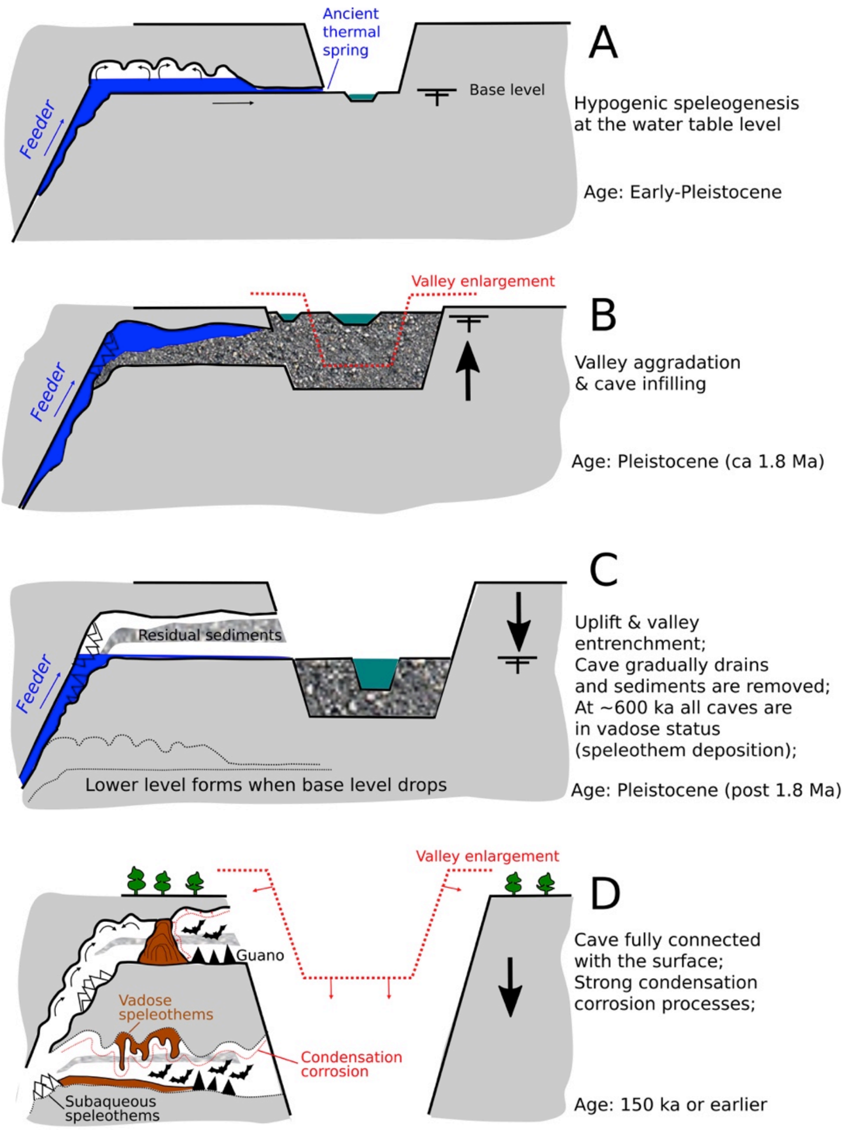

Fig. 13. Evolution of a given level of Toirano caves (especially Colombo and Lower Santa Lucia). A. Horizontal cave connected to base level develops with hypogene upflow and condensation-corrosion in the confined part. B. Fluvial aggradation (Early Pleistocene) rises the base level and fills the entrance passages with coarse fluvial material. C. Subsequent base level drop following the continuous uplift allows reopening of the cave with partial removal of the fluvial filling. D. Because of slope retreat, condensation-corrosion occurs in the still confined portions of the cave through geothermal effect, with more effective corrosion in the entrances accessible to moist external air and bat colonies.

Only in more recent times, at least 150 ka (based on the oldest archaeological findings), but probably much earlier, the entire cave system fully connected with the external atmosphere, initiating the air circulation and local condensation-corrosion processes. All signs of vadose flow visible today are to be connected to recent invasion or interception of small inflows or infiltrations in the pre-existing hypogenic cave system.

The intense condensation-corrosion, still very active today, has erased many of the morphologies and deposits of the original hypogene speleogenetic phase. The presence of large bat colonies appears to have a strong influence on later vadose condensation-corrosion processes, playing an important role in shaping the voids they occupy. Wall retreat by sole condensation-corrosion can be estimated in over 1 metre in the highest caves (Colombo) due to the combined action of air circulation and bat colonies. Condensation-corrosion, however, is also active in more recently opened caves such as Bàsura, and warrants attention in the future for conservational issues.

We suggest taking this study as a guideline for a thorough investigation of cave evolution, based on a correct interpretation of underground morphologies, sustained by geochemical analyses, anchored in time by dating and coherently integrated with surface events.

Acknowledgements

Many thanks to the staff of the Toirano Caves, and especially to Dr. Flavia Toso, local geologist interested in knowing more about the caves, to archaeologist Dr. Marta Zunino, Scientific Director of Toirano Caves, for her availability, enthusiasm and continuous support, to Dr. Elisabetta Starnini, of the University of Pisa, and to the Archaeological Superintendency of Liguria, the Managing Authority of the show caves, and the Municipality of Toirano. Yves Krüger is thanked for his help in fluid inclusion petrography. We are also grateful to Régis Braucher (Aix Marseille University, CNRS) for his support during AMS analyses. ASTER AMS national facility (CEREGE, Aix-en-Provence) is supported by the INSU/CNRS, the ANR through the "Projets thématiques d'excellence" program for the "Équipements d'excellence" ASTER-CEREGE action and IRD".

U/Th dating was supported by grants from the Science Vanguard Research Program of the Ministry of Science and Technology (MOST) (109-2123-M-002-001 to C.-C.S.), the National Taiwan University (109L8926 to C.-C.S.), the Higher Education Sprout Project of the Ministry of Education, Taiwan ROC (109L901001 to C.-C.S.). Thanks to Luca Pisani (Bologna University) for the DTM used in fig. 1. Finally, we are grateful to Dr D. Ballesteros and an anonymous reviewer for their insightful comments.

References

Arobba, D., Boschian, G., Caramiello, R., Giampietri, A., Negrino, F., Tozzi, C., 2008. La grotta del Colombo : indagini geoarcheologiche, palinologiche e sull'industria litica. Toirano e la Grotta della Bàsura. Atti del Convegno, Bordighera, 69-88.

Audra, P., Palmer, A.N., 2015. Research frontiers in speleogenesis. Dominant processes, hydrogeological conditions and resulting cave patterns. Acta Carsologica 44, 315-348.

Audra, P., Barriquand, L., Bigot, J.-Y., Cailhol, D., Caillaud, H., Vanara, N., Nobécourt, J.-C., Madonia, G., Vattano, M., Renda, M., 2016. L'impact méconnu des chauves-souris et du guano dans l'évolution morphologique tardive des cavernes. Karstologia 68, 1-20.

Audra, P., De Waele, J., Bentaleb, I., Chroňáková, A., Krištůfek, V., D'Angeli, I.M., Carbone, C., Madonia, G., Vattano, M., Scopelliti, G., Cailhol, D., Vanara, N., Temovski, M., Bigot, J.-Y., Nobécourt, J.-C., Galli, E., Rull, F., Cailhol, D., 2019. Guano-related phosphate-rich minerals in European caves. International Journal of Speleology 48, 75-105.

Badino, G., 2010. Underground meteorology-"What's the weather underground?". Acta Carsologica 39, 427-448.

Bahain, J.-J., 1993. Datation par résonance de spin électronique (ESR) de carbonates et d'émail dentaire quaternaires - Potentiel et limites. Thesis. Muséum National d'Histoire Naturelle, Paris, 114 p.

Bella, P., Bosák, P., Braucher, R., Pruner, P., Hercman, H., Minár, J., Veselsky, M., Holec, J., Léanni, L., 2019. Multi-level Domica–Baradla cave system (Slovakia, Hungary): Middle Pliocene–Pleistocene evolution and implications for the denudation chronology of the Western Carpathians. Geomorphology 327, 62-79.

Ballesteros, D., Giralt, S., García-Sansegundo, J., Jiménez-Sánchez, M., 2019. Quaternary regional evolution based on karst cave geomorphology in Picos de Europa (Atlantic Margin of the Iberian Peninsula). Geomorphology 336,133-151. https://doi.org/10.1016/j.geomorph.2019.04.002

Boni, A., Cerro, A., Gianotti, R., Vanossi, M., 1971. Note illustrative carta geologica d'Italia. Foglio 92-93. Albenga – Savona. Servizio Geologico d'Italia: Roma.

Bontognali, T.R.R., D'Angeli, I.M., Tisato, N., Vasconcelos, C., Bernasconi, S.M., Grau Gonzales, E.R., De Waele, J., 2016. Mushroom Speleothems: Stromatolites that formed in the absence of phototrophs. Frontiers in Earth Science 4, Article 49.

Cailhol, D., Audra, P., Nehme, C., Nader, F.H., Garašić, M., Heresanu, V., Gucel, S., Charalambidou, I., Satterfield, L., Cheng, H., Edwards, R.L., 2019. The contribution of condensation-corrosion in the morphological evolution of caves in semi-arid regions: preliminary investigations in the Kyrenia Range, Cyprus. Acta Carsologica 48, 5-27.

Calandri, G., 2001. L'evoluzione del carsismo nel Toiranese: nota preliminare. In : Atti V Convegno Speleologico Ligure "Toirano 2000". Toirano, Italy, 117-120.

Calvet, M., Gunnell, Y., Braucher, R., Hez, G., Bourlès, D., Guillou, V., Delmas, M., ASTER Team, 2015. Cave levels as proxies for measuring post-orogenic uplift: Evidence from cosmogenic dating of alluvium-filled caves in the French Pyrenees. Geomorphology 246, 617-633.

Carobene, L., Firpo, M., 2002. Forme terrazzate relitte di genesi marina lungo la costa ligure tra Genova e Savona (Liguria Occidentale). Il Quaternario 15, 53-68.

Carobene, L., Cevasco, A., 2011. A large scale lateral spreading, its genesis and Quaternary evolution in the coastal sector between Cogoleto and Varazze (Liguria-Italy). Geomorphology 129(3-4), 398-411.

Cavallo, C., 1990. Indagine idrogeologica su alcune sorgenti del Toiranese. PhD thesis, Univ. of Genova, 160 p.

Cavallo, C., 2001. Geologia e carsismo del massiccio del Monte Carmo di Loano. Atti V Convegno Speleologico Ligure “Toirano 2000”. Toirano, Italy, 17-21.

Cheng, H., Edwards, R.L., Shen, C.C., Polyak, V.J., Asmerom, Y., Woodhead, J., Hellstrom, J., Wang, Y., Kong, X., Spötl, C., Wang, X., Calvin, A.E., 2013. Improvements in ^{230}Th dating, ^{230}Th and ^{234}U half-life values, and U/Th isotopic measurements by multi-collector inductively coupled plasma mass spectrometry. Earth and Planetary Science Letters 372, 82-91.

Chiesa, R., 2007. La Grotta del Colombo di Toirano (SV): Contributo preliminare alla conoscenza della cavità. In: Atti XX Congresso Nazionale di Speleologia. Iglesias, Italy. Memorie dell’Istituto Italiano di Speleologia 2 (21), 130-138

Citton, P., Romano, M., Salvador, I., Avanzini, M., 2017. Reviewing the upper Pleistocene human footprints from the ‘Sala dei Misteri’ in the Grotta della Bàsura (Toirano, northern Italy) cave: An integrated morphometric and morpho-classificatory approach. Quaternary Science Reviews 169, 50-64.

Clauzon, G., Rubino, J.-L., Suc, J.-P., 1996. Les rias pliocènes du Var et de Ligurie: comblement sédimentaire et évolution géodynamique. Excursion commune Groupe français de géomorphologie et Groupe français d’étude du Néogène, 109 p.

Columbu, A., De Waele, J., Forti, P., Montagna, P., Picotti, V., Pons-Branchu, E., Hellstrom, J., Bajo, P., Drysdale, R., 2015. Gypsum caves as indicators of climate-driven river incision and aggradation in a rapidly uplifting region. Geology 43, 539-542.

Columbu, A., Chiarini, V., De Waele, J., Drysdale, R.N., Woodhead, J., Hellstrom, J., Forti, P., 2017. Late quaternary speleogenesis and landscape evolution in the northern Apennine evaporite areas. Earth Surface Processes and Landforms 42, 1447-1459.

Columbu, A., Sauro, F., Lundberg, J., Drysdale, R.N., De Waele, J., 2018. Palaeoenvironmental changes recorded by speleothems of the southern Alps (Piani Eterni, Belluno, Italy) during four interglacial to glacial climate transitions. Quaternary Science Reviews 197, 319-335.

Columbu, A., Spötl, C., De Waele, J., Yu, T.L., Shen, C.C., Gázquez, F., 2019. A long record of MIS 7 and MIS 5 climate and environment from a western Mediterranean speleothem (SW Sardinia, Italy). Quaternary Science Reviews 220, 230-243.

Columbu, A., Chiarini, V., Spötl, C., Benazzi, S., Hellstrom, J., Cheng, H., De Waele, J., 2020. Speleothem record attests to stable environmental conditions during Neanderthal-Modern Human turnover in Southern Italy. Nature Ecology & Evolution 4, 1188-1195.

Dandurand, G., Duranthon, F., Jarry, M., Stratford, D.J., Bruxelles, L., 2019. Biogenic corrosion caused by bats in Drotsky's Cave (the Gcwihaba Hills, NW Botswana). Geomorphology 327, 284-296.

D'Angeli, I.M., Carbone, C., Nagostinis, M., Parise, M., Vattano, M., Madonia, G., De Waele, J., 2018. New insights on secondary minerals from Italian sulfuric acid caves. International Journal of Speleology 47, 271-291.

D'Angeli, I.M., Parise, M., Vattano, M., Madonia, G., Galdenzi, S., De Waele, J., 2019a. Sulfuric acid caves of Italy: A review. Geomorphology 333, 105-122.

D'Angeli, I.M., Nagostinis, M., Carbone, C., Bernasconi, S.M., Polyak, V.J., Peters, L., McIntosh, B., De Waele, J., 2019b. Sulfuric acid speleogenesis in the Majella Massif (Abruzzo, Central Apennines, Italy). Geomorphology 333, 167-179.

De Waele, J., Plan, L., Audra, P., 2009. Recent developments in surface and subsurface karst geomorphology: An introduction. Geomorphology 106, 1-8.

De Waele, J., Audra, P., Madonia, G., Vattano, M., Plan, L., D'Angeli, I.M., Bigot, J.-Y., Nobécourt, J.C., 2016. Sulfuric acid speleogenesis (SAS) close to the water table: examples from southern France, Austria, and Sicily. Geomorphology 253, 452-467.

De Waele, J., D'Angeli, I.M., Bontognali, T., Tuccimei, P., Scholz, D., Jochum, K.P., Columbu, A., Bernasconi, S.M., Fornós, J.J., Grau González, E.R., 2018 Speleothems in a north Cuban cave register sea level changes and Pleistocene uplift rates. Earth Surface Processes and Landforms 43, 2313-2326.

Fanucci, F., 1985. La Grotta preistorica della Bàsura. Rivista di Studi Liguri 51, 341-343.

Fanucci, F., Firpo, M., Ramella, A., 1987. Genesi ed evoluzione di piane costiere del Mediterraneo: esempi di piccole piane della Liguria. Geografia Fisica e Dinamica Quaternaria 10, 193-203.

Ferraris, F., Firpo, M., Pazzaglia, F.J., 2012. DEM analyses and morphotectonic interpretation: The Plio-Quaternary evolution of the eastern Ligurian Alps, Italy. Geomorphology 149, 27-40.

Ford, D.C., Williams, P.W., 2007. Karst Hydrogeology and Geomorphology. John Wiley & Sons: Chichester.

Gázquez, F., Columbu, A., De Waele, J., Breitenbach, S.F., Huang, C.R., Shen, C.C., Lu, Y., Calaforra, J.-C., Mleneck-Vautravers, M.J., Hodell, D.A., 2018. Quantification of paleo-aquifer changes using clumped isotopes in subaqueous carbonate speleothems. Chemical Geology 493, 246-257.

Gruppo Speleologico Cycnus & Delegazione Speleologica Ligure, 2001. Speleologia e carsismo del Toiranese". Atti V Convegno Speleologico Ligure "Toirano 2000". Toirano, Italy.

Hellstrom, J., 2003. Rapid and accurate U/Th dating using parallel ion-counting multi-collector ICP-MS. Journal of Analytical Atomic Spectrometry 18, 1346-1351.

Klimchouk, A.B., 2007. Hypogene speleogenesis: hydrogeological and morphogenetic Perspective. – National Cave and Karst Research Institute, Special Paper 1, 106 pp.

Krüger, Y., Marti, D., Staub, R.H., Fleitmann, D., Frenz, M., 2011. Liquid–vapour homogenisation of fluid inclusions in stalagmites: Evaluation of a new thermometer for palaeoclimate research. Chemical Geology 289, 39-47.

Klanica, R., Kadlec, J., Tábořík, P., Mrlina, J., Valenta, J., Kováčiková, S., Hill, G.J., 2020. Hypogenic Versus Epigenic Origin of Deep Underwater Caves Illustrated by the Hranice Abyss (Czech Republic) - The World's Deepest Freshwater Cave. Journal of Geophysical Research: Earth Surface 125.9, e2020JF005663.

Klimchouk, A.B., Palmer, A.N., De Waele, J., Auler, A.S., Audra, P., 2017. Hypogene karst regions and caves of the world. Springer: Cham.

Leél-Őssy, S., 2017. Caves of the Buda Thermal karst. In: Klimchouk, A.B., Palmer, A.N., De Waele, J., Auler, A.S., Audra, P. (Eds.) Hypogene Karst Regions and Caves of the World, Cave and Karst Systems of the World. Springer, Cham. https://doi.org/10.1007/978-3-319-53348-3_18

Lundberg, J., McFarlane, D.A., 2009. Bats and bell holes: the microclimatic impact of bat roosting, using a case study from Runaway Bay Caves, Jamaica. Geomorphology 106, 78-85 http://dx.doi.org/10.1016/j.geomorph.2008.09.022.

Lundberg, J., McFarlane, D.A., 2012. Post-speleogenetic biogenic modification of Gomantong Caves, Sabah, Borneo. Geomorphology 157-158, 153-168. https://doi.org/10.1016/j.geomorph.2011.04.043

Lundberg, J., McFarlane, D.A., 2015. Microclimate and niche constructionism in tropical bat caves: A case study from Mount Elgon, Kenya. In: Feinberg, J., Gao, Y., Alexander, E.C. Jr. (Eds.). Caves and Karst across Time, Geological Society of America Special Paper, G, http://dx.doi.org/10.1130/2015.2516(18).

Marini, M., 2004. Carta geologica del Pliocene ligure di Albenga (Alpi Marittime – Provincia di Savona), 1:25.000. SELCA: Firenze.

McDermott, F., 2004. Palaeo-climate reconstruction from stable isotope variations in speleothems: a review. Quaternary Science Reviews 23, 901-918.

Menardi Noguera, A., 1984. Nuove osservazioni sulla struttura del massiccio del Monte Carmo (Alpi Liguri). Bollettino della Società Geologica Italiana 103, 189-203.

Molleson, T.I., Oakley, K.P., Vogel, J.C., 1972. The antiquity of human footprints of Tana della Bàsura. Journal of Human Evolution 1, 467-471.

Nehme, C., Farrant, A., Ballesteros, D., Todisco, D., Rodet, J., Sahy, D., Grappone, J.M., Staigre, J.C., Mouralis, D., 2020. Reconstructing fluvial incision rates based on palaeo-water tables in chalk karst networks along the Seine valley (Normandy, France). Earth Surface Processes and Landforms 45, 1860-1876. https://doi.org/10.1002/esp.4851

Palmer, A.N., 1987. Cave levels and their interpretation. National Speleological Society Bulletin 49, 50-66.

Palmer, A.N., 2007. Cave geology. Cave Books: Dayton (OH).

Pennos, C., Lauritzen, S.E., Vouvalidis, K., Cowie, P., Pechlivanidou, S., Gkarlaouni, C., Styllas, M., Tsourlos, P., Mouratidis, A., 2019. From subsurface to surface: a multidisciplinary approach to decoding uplift histories in tectonically-active karst landscapes. Earth Surface Process and Landforms 44,1710-1721. https://doi.org/10.1002/esp.4605

Pérez-Mejías, C., Sancho, C., Gàzquez, F., Moreno, A., Bartolomé, M., Osácar, M.C., Cheng, H., 2019. Insights into the speleogenesis of Ejulve cave (Iberian Range, NE Spain): quaternary hydrothermal karstification?. Journal of Iberian Geology 45, 511-527.

Piccini, L., De Waele, J., Galli, E., Polyak, V.J., Bernasconi, S.M., Asmerom, Y., 2015. Sulphuric acid speleogenesis and landscape evolution: Montecchio cave, Albegna river valley (Southern Tuscany, Italy). Geomorphology 229, 134-143.

Pirouelle, F., 2006. Contribution méthodologique à la datation, par les méthodes uranium-thorium (U-Th) et résonance de spin électronique (ESR), de sites moustériens de Ligurie, de France et de Belgique. PhD Thesis, Muséum National d’Histoire Naturelle, Paris, 442 p.

Plan, L., Tschegg, C., De Waele, J., Spötl, C., 2012. Corrosion morphology and cave wall alteration in an Alpine sulfuric acid cave (Kraushöhle, Austria). Geomorphology 169-170, 45-54. https://doi.org/10.1016/j.geomorph.2012.04.006

Pozzi, J.P., Rousseau, L., Falguères, C., Mahieux, G., Deschamps, P., Shao, Q., Kachi, D., Bahain, J.-J., Tozzi, C., 2019. U-Th dated speleothem recorded geomagnetic excursions in the Lower Brunhes. Scientific Reports 9, 1-8.

Rohling, E.J., Foster, G.L., Grant, K.M., Marino, G., Roberts, A.P., Tamisiea, M.E., Williams, F., 2014. Sea-level and deep-sea-temperature variability over the past 5.3 million years. Nature 508(7497), 477-482.

Sarigu, S., 2001. Il carsismo del complesso turistico di Toirano: descrizione strutturale, morfologica e concrezionale. Ipotesi genetica per la grotta della Bàsura", Atti V Convegno Speleologico Ligure "Toirano 2000". Toirano, Italy, 149-156.

Sauro, F., Mecchia, M., Piccini, L., De Waele, J., Carbone, C., Columbu, A., Pisani, L., Vergara, F., 2019. Genesis of giant sinkholes and caves in the quartz sandstone of Sarisariñama tepui, Venezuela. Geomorphology 342, 223-238.

Sauro, F., Mecchia, M., Tringham, M., Arbenz, T., Columbu, A., Carbone, C., Pisani, L., De Waele, J., 2020. Speleogenesis of the world's longest cave in hybrid arenites (Krem Puri, Meghalaya, India). Geomorphology 350, 107-160.

Sasowsky, I.D., 1998. Determining the age of what is not there. Science 279, 1874-1874.

Shen, C.C., Wu, C.C., Cheng, H., Edwards, R.L., Hsieh, Y.T., Gallet, S., Chang, C.C., Li, T.Y., Lam, D.D., Kano, A., Hori, M., Spötl, C., 2012. High-precision and high-resolution carbonate 230Th dating by MC-ICP-MS with SEM protocols. Geochimica et Cosmochimica Acta 99, 71-86.

Shen, G., 1985. Datation des planchers stalagmitiques de sites acheuléens en Europe par les méthodes des déséquilibres des familles de l'uranium et contribution méthodologique. PhD Thesis, Université Pierre et Marie Curie, Paris VI, 162 p.

Soulet, Q., Migeon, S., Gorini, C., Rubino, J,-L,, Raisson, F., Bourges, P., 2016. Erosional versus aggradational canyons along a tectonically-active margin: The northeastern Ligurian margin (western Mediterranean Sea). Marine Geology 382,17-36. http://dx.doi.org/10.1016/j.margeo.2016.09.015

Temovski, M., Audra, P., Mihevc, A., Spangenberg, J.E., Polyak, V., McIntosh, W., Bigot, J.-Y., 2013. Hypogenic origin of Provalata Cave, Republic of Macedonia: a distinct case of successive thermal carbonic and sulfuric acid speleogenesis. International Journal of Speleology 42, 235-246. https://doi.org/10.5038/1827-806X.42.3.7

Tisato, N., Sauro, F., Bernasconi, S.M., Bruijn, R.H., De Waele, J., 2012. Hypogenic contribution to speleogenesis in a predominant epigenic karst system: a case study from the Venetian Alps, Italy. Geomorphology 151, 156-163. https://doi.org/10.1016/j.geomorph.2012.01.025

Tremaine, D.M., Froelich, P.N., Wang, Y., 2011. Speleothem calcite farmed in situ: Modern calibration of $\delta^{18}O$ and $\delta^{13}C$ paleoclimate proxies in a continuously-monitored natural cave system. Geochimica et Cosmochimica Acta 75, 4929-4950.